Count Variables with Locally Explosive Patterns

Joann Jasiak *, Elaheh Zarabi †

June 20, 2026
preliminary version

Abstract

This paper shows that count variables of sentiment display locally explosive patterns, such as bubbles and spikes and can be modeled using the noncausal or mixed causal-noncausal integer autoregressive (MIAR) processes. We examine the performance of the existing estimators of these models and consider the Indirect Inference method as an alternative approach, given that the log-likelihood function of the MIAR model is not tractable. We show that the Indirect Inference estimator based on the continuously-valued mixed causal-noncausal process as an auxiliary model in application to mixed MIAR processes leads to significant bias reduction compared to the GMM. In addition, the Indirect Inference provides simple plug-in estimators of the pure causal INAR(1) and noncausal integer processes based on the Gaussian AR(1) as an auxiliary model. The approach is illustrated by simulations and an application to tweet counts on Apple and GameStop reported by Bloomberg.

Keywords: Sentiment, Noncausal Process, Count Process, Bubble

*York University, Canada,*e-mail*: jasiakj@yorku.ca
†York University, Canada, *e-mail*: jasiakj@yorku.ca
The authors gratefully acknowledge financial support of the Natural Sciences and Engineering Research Council of Canada (NSERC) and thank Christian Gourieroux and Yang Lu for helpful comments.

1 Introduction

The sentiment variables reported by Bloomberg are count processes with serial dependence. Therefore, they can be represented by integer count variable models to solve the problem of non-negativity and to ensure integer-valued forecasts. These integer-valued sentiment processes need to be distinguished from continuously-valued sentiment indices based on surveys of inflation expectations, economic uncertainty, input and output price expectations, as well as other indices like economic policy uncertainty (EPU) index. A popular dynamic model for count processes is the Integer Autoregressive of order 1 (INAR(1)) model [see, e.g., McKenzie (1985), Al-Osh and Alzaid (1987)]. Recently, count processes with locally explosive patterns have received attention in the literature. Gouriéroux and Lu (2021) introduced a noncausal Integer Autoregressive process of order 1 (noncausal INAR(1)) and applied it to hourly rainfall data displaying bubbles with a vertical crash. Pei et al. (2025) extended the noncausal INAR(1) to a class of mixed causal-noncausal count processes for applications to the counts of stock trades on major stock exchange markets, where bubbles burst at a slower pace. An important difference between these two classes of processes is that the pure causal and noncausal INAR(1) are Markov, while the mixed causal-noncausal integer autoregressive process (MIAR henceforth) is not. Another difference concerns the estimation methods. Pei et al. (2025) show that the MIAR can be estimated by the Generalized Method of Moments (GMM) whereas the Maximum Likelihood (ML) is not tractable. In contrast, the causal or noncausal INAR(1) models can be estimated by the Maximum Likelihood as well as by the GMM. However, the performance of the GMM in application to MIAR processes is shown to depend on the choice of moments, which can be difficult. Pei et al. (2025) report a bias-variance trade-off resulting from a choice of two different set of moments, which implies that an arbitrary choice of moments affects the outcomes.

Our objective is to show that simulation-based methods can be used for inference on MIAR processes. In particular, we explore the Indirect Inference. Our results indicate that the Indirect Inference estimator is applicable to both the pure and mixed autoregressive integer processes, unlike the maximum likelihood. Moreover, it leads to significant bias reduction in the mixed MIAR processes, compared to the GMM.

In addition, we explore the estimation of pure causal and noncausal integer processes. We show that Indirect Inference provides simple plug-in estimators of pure causal INAR(1) and noncausal integer processes, based on the Gaussian AR(1) as an auxiliary model. This procedure considerably simplifies inference on these popular count data models.

The paper is organized as follows. Section 2 describes the data and Section 3 presents the models available in the literature, their estimation methods and a simulation experiment illustrating their performance. Section 5 introduces the simulation-based inference for sentiment variables with locally explosive features and a simulation study. Section 6 contains a simulation study and an application to tweet counts on Apple and GameStop reported by Bloomberg. Section 7 concludes. Appendices A and B present additional technical and empirical results.

2 Data Description

The sentiment data collected by Bloomberg are integer-valued. These sentiment variables represent the counts of tweets and can display locally explosive patterns. We consider two datasets of tweets on Apple and GameStop stocks which are described below.

2.1 The Negative Tweets series

We examine two time series of daily numbers of negative tweets regarding Apple Inc. (stock ticker $AAPL$) from January 1, 2023 to February 3, 2024 and GameStop Corp. (stock ticker GME) between October 1, 2020 and May 5, 2022. These sentiment variables represent the raw frequency of tweets that Bloomberg's proprietary Natural Language Processing (NLP) engine classifies as having a "Negative" polarity. The summary statistics are given in Table 1.

Table 1: Summary Statistics of Sentiment Count Variables

Statistic	AAPL Negative Tweet	GME Negative Tweet
Number Of Observation	285	435
Min	2	3
Max	305	5960
Mean	31	230
Median	20	69
Variance	1407	311706
Range	303	5957
Dispersion Ratio(variance/mean)	44	1614

We observe a slight asymmetry and a large difference between the variance and the mean for both series. Figures 1 and 2 show the time series of numbers of negative tweets regarding Apple and GameStop stocks, respectively.

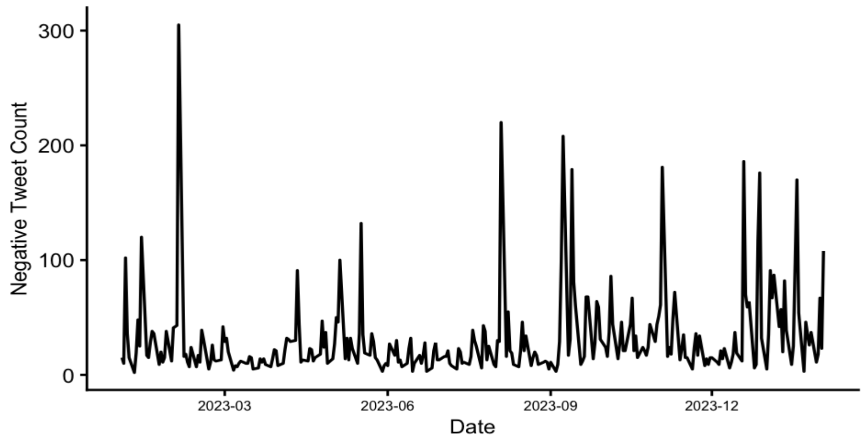

Figure 1: AAPL -Daily numbers of negative tweets

The series of tweets on Apple in Figure 1 has an average of 31 tweets per day. Occasionally the tweets suddenly ”explode”, like for example in early February 2023, when the negative tweets regarding Apple suddenly jumped from 40 to 305 over three days, and then fell to about 15 tweets on the following day. This locally explosive negative reaction was triggered by the first decline in quarterly revenue reported by the company since 2019. Similar patterns that occurred later show how public feeling about this stock shifts rapidly in response to news such as lack of innovation and technical problems like overheating.

In Figure 2 presenting the negative tweets on GME over time, we observe that before year 2021, GME stock was not discussed much in social media, and had nearly zero negative sentiment. However, a bubble with a peak of about 6000 occurred in early 2021, followed by several smaller spikes later during that year.

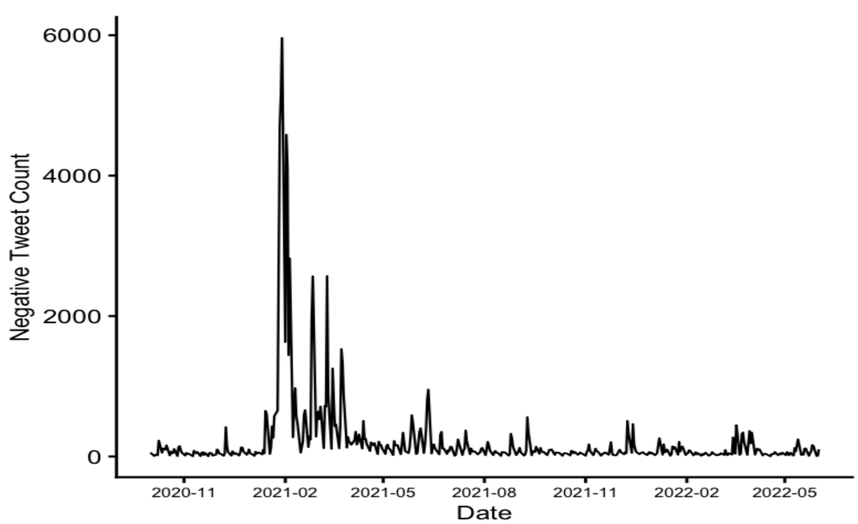

Figure 2: GME -Daily numbers of negative tweets

Overall, the sentiment count series exhibits bubbles and spikes, which are nonlinear dynamic patterns, suggesting the presence of both causal and anticipatory (noncausal) effects.

In order to identify bubbles and other local explosive pattern in noncausal models of counts, the integer-valued data should not be Poisson distributed to ensure the identification of noncausal components (Gouriéroux and Lu (2021)). We test the data for Poisson distribution by calculating the dispersion ratio, and conduct the Cameron–Trivedi overdispersion test. The dispersion ratio, reported in the last row of Table 1 shows that the variances of both tweet series are greater than their means. Hence, we reject the Poisson assumption that the variance is equal to the mean in both samples. The test statistics for AAPL is 3.91 with a p-value of 4.5×10^{-5} and the test statistic for GME is 3.06, p-value 0.001. Consequently, the null hypothesis of equidispersion is rejected in both samples.

The empirical densities of both tweet series are illustrated in Figures 6 and 7 of Appendix B.1., respectively. Each density is compared to the Poisson distribution to visualize the differences.

To illustrate the serial dependence in each series, Figure 8 in Appendix B.1. shows their autocorrelation functions (ACF) which reveal significant serial correlation in both tweet count series.

3 Dynamic Count Models

In this section, we first review the literature on causal and noncausal integer autoregressive INAR(1) processes and on the mixed integer causal-noncausal MIAR model. Next, we describe the estimation methods proposed in the existing literature and illustrate their performance in a simulation study.

3.1 Causal INAR(1) process and its moving average representation

The causal INAR(1) model [see, e.g. McKenzie (1985), Al-Osh and Alzaid (1987), Alzaid and Al-Osh (1990), Gourieroux and Jasiak (2004)] represents the past-dependent dynamics of counts. It is defined as follows:

Definition 1 (Causal INAR(1)). *The process (X_t) is causal INAR(1) if it has the representation:*

$$X_{t+1} = \sum_{i=1}^{X_t} Z_{i,t+1} + \varepsilon_{t+1}, \quad \forall t \in \mathbb{Z}, \tag{1}$$

where latent counts $Z_{i,t+1}$, $i = 1, 2...,$, $t = 1, ...,$ are i.i.d. in i and t and Bernoulli(α) distributed with probability parameter $\alpha \in [0, 1)$, independent of $\underline{X}_t = \{X_t, X_{t-1}, \ldots\}$. The integer-valued errors ε_{t+1} are i.i.d., and independent of both $\underline{X}_t$ and $Z_{i,t+1}$ for all i.

The stationarity condition of the causal INAR(1) is given by Foster and Williamson (1971) in Theorem 1(iii): There exists a strictly stationary INAR(1) process, which is almost surely finite if the distribution of (ε_t) satisfies:

$$\int_0^1 \frac{1 - E[s^{\varepsilon_t}]}{1 - s} \, ds < \infty. \tag{2}$$

This stationarity condition concerns the tails of the marginal distribution of ε_t. It is automatically satisfied when $E(\varepsilon_{t+1}) < \infty$.

The causal INAR(1) model has a one-sided moving average representation [Gouriéroux and Lu (2021), Section 3.5]:

$$X_t = \varepsilon_t + \varepsilon_{t-1}(t) + \varepsilon_{t-2}(t) + \cdots , \tag{3}$$

where the joint distribution of $(\varepsilon_s(t))_{t \geq s}$ is such that the conditional distribution of $\varepsilon_s(t+1)$ given $\varepsilon_s(t)$ is binomial with probability $\alpha \in [0, 1)$, that is $\varepsilon_s(t+1) = \sum_{i=1}^{\varepsilon_s(t)} Z_{i,s,t+1}$, $\forall t \geq s$, where $\varepsilon_s(s) = \varepsilon_s$, and $Z_{i,s,t+1}$ are i.i.d. Bernoulli(α) distributed, independent of $\varepsilon_s(t), \varepsilon_s(t-1), \ldots$ The sequences $(\varepsilon_s(t))_{t \geq s}$ are independent for different s.

An informal thinning representation is (Gouriéroux and Lu, 2021):

$$X_t \stackrel{d}{=} \varepsilon_t + \alpha \circ \varepsilon_{t-1} + \alpha^2 \circ \varepsilon_{t-2} + \cdots , \tag{4}$$

where $\stackrel{d}{=}$ denotes the equality in distribution and $\circ$ denotes the (stochastic) thinning operator $\alpha \circ$ for a non-negative variable Y is defined as $\sum_{i=1}^{Y} Z_i$, with (Z_i) are i.i.d. Bernoulli distributed with parameter α.

3.2 Noncausal INAR(1) process

The noncausal INAR(1) process is obtained by time-reversing the causal INAR(1) (Gouriéroux and Lu, 2021). It represents the forward looking temporal dependence in count variables and models integer processes with bubbles that end in a vertical crash. It is defined as follows:

Definition 2 (Noncausal INAR(1) [Gouriéroux and Lu (2021)]). *The process (X_t) is noncausal INAR(1) if it can be written as:*

$$X_t = \sum_{i=1}^{X_{t+1}} Z^*_{i,t} + \tilde{\varepsilon}_t, \quad \forall t \in \mathbb{Z}, \tag{5}$$

where $\tilde{\varepsilon}_t$, $t = 1, \ldots$, are independent of $\overline{X_{t+1}} = \{X_{t+1}, X_{t+2}, \ldots\}$, and are i.i.d. in t. Variables $Z^*_{i,t}$ $i = 1, 2, \ldots$, $t = 1, \ldots$, are i.i.d. in i and t and are Bernoulli (β) distributed and are independent of $\overline{X_{t+1}}$ and $\tilde{\varepsilon}_t$.

Gouriéroux and Lu (2021) show that there exists a strictly stationary noncausal INAR(1) process, which is almost surely finite if eq.(2) holds.

The noncausal INAR(1) has a one-sided moving average representation (Gouriéroux and Lu, 2021):

$$X_t = \tilde{\varepsilon}_t + \tilde{\varepsilon}_{t+1}(t) + \tilde{\varepsilon}_{t+2}(t) + \cdots , \tag{6}$$

where

$$\tilde{\varepsilon}_t(s-1) = \sum_{i=1}^{\tilde{\varepsilon}_t(s)} Z^*_{i,s,t}, \quad \forall s \leq t, \text{ with } \tilde{\varepsilon}_t(t) = \tilde{\varepsilon}_t. \tag{7}$$

where $Z^*_{i,s,t}, i = 1, 2, \ldots$ are i.i.d. Bernoulli (β) distributed and are independent of $\tilde{\varepsilon}_t(s)$. The departure counts $\tilde{\varepsilon}_s$, $s \in \mathbb{Z}$ are i.i.d. and independent of $Z^*_{i,s,t}$.

An informal thinning representation is (Gouriéroux and Lu, 2021):

$$X_t \stackrel{d}{=} \tilde{\varepsilon}_t + \beta \circ \tilde{\varepsilon}_{t+1} + \beta^2 \circ \tilde{\varepsilon}_{t+2} + \cdots , \tag{8}$$

where the notation and interpretation are similar to those in (4).

3.3 Mixed causal-noncausal process

The mixed causal-noncausal integer autoregressive MIAR(1,1) model allows for a slower than vertical rate of bubble decline and represents integer time series with asymmetric bubbles. This process combines the pure causal and noncausal INAR(1) processes. However, unlike these pure processes, it is not Markov, neither in the calendar nor in reverse time (Pei et al., 2025).

Definition 3 (Mixed integer causal-noncausal MIAR(1,1), (Pei et al., 2025))**.** *The count process* (X_t) *is mixed causal-noncausal integer autoregressive, denoted MIAR(1,1), if*

$$X_t = \varepsilon_t + \sum_{k=1}^{\infty} \varepsilon_{t-k}(t) + \sum_{k=1}^{\infty} \varepsilon_{t+k}(t), \quad \forall t \in \mathbb{Z}, \tag{9}$$

where (ε_t) *is an i.i.d. sequence of nonnegative integer variables, and the doubly indexed innovations* $(\varepsilon_s(t))_{s,t}$ *are defined via forward and backward binomial thinning with probabilities* α *and* β *as follows.*
For each $s \in \mathbb{Z}$*, sequence* $(\epsilon_s(t))_{t>s}$ *is defined forward as:*

$$\varepsilon_s(t+1) = \sum_{i=1}^{\varepsilon_s(t)} Z_{i,s,t}, \quad t \geq s, \tag{10}$$

For each $t \in \mathbb{Z}$*, sequence* $(\epsilon_t(s))_{s<t}$ *is defined backward as:*

$$\varepsilon_t(s-1) = \sum_{j=1}^{\varepsilon_t(s)} Z^*_{j,s,t}, \quad s \leq t, \tag{11}$$

with $Z_{i,s,t} \sim$ *Bernoulli*(α) *and* $Z^*_{j,s,t} \sim$ *Bernoulli*(β) *are i.i.d. across i,s,t. For* $s \in \mathbb{Z}, \varepsilon_s(s) = \varepsilon_s$ *is an i.i.d. sequence across different cohorts* s*.*

The informal thinning representation is (Pei et al. (2025)):

$$X_t \overset{d}{=} \varepsilon_t + \left(\alpha \circ \varepsilon_{t-1} + \alpha^2 \circ \varepsilon_{t-2} + \cdots\right) + \left(\beta \circ \varepsilon_{t+1} + \beta^2 \circ \varepsilon_{t+2} + \cdots\right)$$

The parameters α and β are the backward and forward thinning parameters, respectively. When either one of them vanishes, a pure causal or non-causal process is obtained.

When the parameters α and β are strictly less than 1, the stationarity condition of the pure noncausal INAR(1) and mixed MIAR(1,1) processes is the same as the stationarity condition (eq.(2)) of the causal INAR process [see, Pei et al. (2025), Proposition 4].

An expression of the mixed integer model analogous to the pure causal and noncausal INAR(1) models:

$$X_t = \sum_{i=1}^{X_{t-1}} Z_{i,t} + \sum_{i=1}^{X_{t+1}} Z^*_{i,t} + \epsilon_t$$

where $Z_{i,t}$, $Z^*_{i,t}$ are independent of one another and of ϵ_t **is not equivalent** to that in Pei et al. (2025). The model defined by Pei et al. (2025) in equations (9-11), Section 3.3, and considered in this paper is:

$$X_t = [u_t + \varepsilon_t] + v_{t+1} \equiv [\varepsilon_t + v_{t+1}] + u_t \tag{12}$$

It implies that the process can be written as the sum of a causal INAR(1) $u_t + \varepsilon_t$ and a "thinned" noncausal component v_{t+1}, or the sum of a noncausal INAR(1) $\varepsilon_t + v_{t+1}$ and a thinned component u_t.

When the errors of the MIAR(1,1) are Poisson distributed with parameter λ, then X_{t+1}, X_t and X_t, X_{t+1} have the same distribution and the parameters α and β cannot be identified. This result is given in Proposition 7, of Pei et al. (2025) who show that the Poisson distribution of (ε_t) implies the lack of identification of the noncausal dynamics[1] [see also Appendix A.1]. When the errors have a Negative Binomial distribution, i.e. $\varepsilon_t \sim \mathcal{NB}(r,p)$, and $\alpha \neq \beta$, then the distribution of X_t, X_{t+1} is different from the distribution of X_{t+1}, X_t, the process (X_t) is time-irreversible, and the parameters α and β can be distinguished [Pei et al. (2025)]. In practice, the errors of the causal or non-causal INAR(1) and MIAR(1,1) models can be assumed to follow a $\mathcal{NB}(r,p)$ distribution to accommodate the overdispersion.

3.4 Maximum likelihood Estimation of INAR(1) Processes

The pure causal and noncausal INAR(1) processes can be estimated by the conditional Maximum Likelihood (ML) assuming, for example, that the errors have a Negative Binomial distribution. Then, ε_t is a causal (resp. noncausal) innovation in the pure causal (resp. noncausal) models and follows a Negative Binomial distribution, $\varepsilon_t \sim \text{NB}(r,p)$, which provides a robust statistical framework for handling overdispersed count data. The probability mass function (pmf) for the innovation process is given by:

$$P_{\text{NB}}(\varepsilon_t = k \mid r, p) = \binom{k+r-1}{k} p^r (1-p)^k, \quad k = 0, 1, 2, \ldots \tag{13}$$

where k is the number of failures, $r > 0$ is the number of successes, and $p \in (0,1)$ is the probability of success in each experiment. Depending on the model, the parameter vector to be estimated is defined as $\theta = (\alpha, r, p)$, where $\alpha \in [0,1]$ is the causal thinning parameter, or as $\theta = (\beta, r, p)$, $\beta \in [0,1]$ is the noncausal thinning parameter; (r,p) are the parameters of the innovation distribution.

The log-likelihood function $\log L(\theta)$ for $X_t,\ t = 1, ..., T$ observations on the pure causal INAR(1) model is the sum of the conditional log-pmf's over $t = 1, ..., T$, as shown in Al-Osh and Alzaid (1987). The log-likelihood function is written as:

$$\log L(\theta) = \sum_{t=2}^{T} \log \left[\sum_{i=0}^{M_{1,t}} \mathcal{B}(i; x_{t-1}, \alpha) \cdot P_{\text{NB}}(x_t - i \mid r, p) \right], \tag{14}$$

where $\mathcal{B}(i; n, \alpha) = \binom{n}{i} \alpha^i (1-\alpha)^{n-i}$ denotes the Binomial pmf, where i is the number of successes, n is the total number of trials, and the summation limit is defined as: $M_{1,t} = \min(x_{t-1}, x_t)$ for the causal INAR(1). For the noncausal INAR(1), the log-likelihood function is:

[1] i.e. the parameters α and β are only identifiable up to a permutation [Pei et al. (2025), Section 3.2].

$$\log L(\theta) = \sum_{t=1}^{T-1} \log \left[\sum_{j=0}^{M_{2,t}} \mathcal{B}(j; x_{t+1}, \beta) \cdot P_{\text{NB}}(x_t - j \mid r, p) \right] \tag{15}$$

with $M_{2,t} = \min(x_{t+1}, x_t)$ for the noncausal INAR(1).

For the MIAR(1,1) model, the log-likelihood function is not tractable [Pei et al. (2025), Section 5.1] and the estimation method suggested by Pei et al. (2025) is the Generalized Method of Moments.

3.5 Generalized Method of Moments for INAR(1) and MIAR(1,1) Processes

As an alternative to the ML, a Generalized Method of Moments (GMM) can be applied to count processes Gouriéroux and Lu (2021), Pei et al. (2025). Unlike the ML, the GMM is applicable to the mixed causal-noncausal integer autoregressive MIAR(1,1) process in addition to the pure INAR(1) processes, as shown in Pei et al. (2025). It minimizes the distance between the empirical and theoretical moments derived from the joint probability generating function (pgf) of the process. The joint pgf of (X_t, X_{t+1}) provides a convenient and informative set of moment conditions, since it fully characterizes the joint distribution. The difficulty is in determining how many and which among the infinity of moment conditions should be used. (Pei et al., 2025) consider a finite grid, and for each element of the grid $(u_k, v_k) \in V \times V$, the corresponding moment condition is defined as:

$$h_k(X_t, X_{t+1}, \theta) = E_\theta \left[u_k^{X_t} v_k^{X_{t+1}} \right] - u_k^{X_t} v_k^{X_{t+1}}, \qquad k = 1, \dots, |V|^2. \tag{16}$$

The GMM estimator $\hat{\theta}_T$ is obtained by minimizing a quadratic form in the sample average of these moment conditions (Pei et al., 2025),

$$\hat{\theta}_T = \arg\min_\theta \left(\frac{1}{T-1} \sum_{t=1}^{T-1} h(X_t, X_{t+1}, \theta) \right)' W \left(\frac{1}{T-1} \sum_{t=1}^{T-1} h(X_t, X_{t+1}, \theta) \right), \tag{17}$$

where W is a symmetric positive definite weighting matrix. The optimal weighting matrix is given by $W = \Omega^{-1}(\theta_0)$, where $\Omega(\theta_0) = E_{\theta_0}[h(X_t, X_{t+1}, \theta_0) h(X_t, X_{t+1}, \theta_0)'] = Var_{\theta_0}(u_k X_t v_k X_{t+1})$ and is illustrated in the next Section.

3.6 Illustration

In this section we explore the performance of the ML and GMM estimators presented in the previous section in simulation experiments.

To simulate a mixed causal noncausal integer autoregressive MIAR(1,1) process defined in equation (9), with i.i.d. errors and a Negative Binomial error distribution, we use the following algorithm:

Simulation Algorithm of MIAR(1,1)

The approach is based on a simulating a $(T \times T)$ matrix of i.i.d innovations starting from the main diagonal:
Step 1: Simulate:

$$\varepsilon_s \sim \text{NB}(r, p), \quad s = 1, \dots, T.$$

Step 2: For each innovation time s, set $\varepsilon_s(s) = \varepsilon_s$.

Step 3: Causal thinning in forward time direction:

$$\varepsilon_s(t) \mid \varepsilon_s(t-1) \sim \text{Binomial}(\varepsilon_s(t-1), \alpha), \quad s = 1, \dots, T, \quad t = s+1, \dots, T.$$

Step 4: Noncausal thinning in backward time direction:

$$\varepsilon_s(t) \mid \varepsilon_s(t+1) \sim \text{Binomial}(\varepsilon_s(t+1), \beta), \quad s = 1, \dots, T, \quad t = s-1, \dots, 1.$$

Step 5: Obtain the simulated count process X_t by summing over all innovation times s:

$$X_t = \sum_{s=1}^{T} \varepsilon_s(t), \quad t = 1, \dots, T.$$

Next, we use the simulated samples to study the performance of the estimators. We consider three model specifications: the purely causal, the purely noncausal, and the mixed causal-noncausal process. For each scenario, we analyze two sample sizes $T = 1000$ and $T = 2000$, and perform $R = 100$ independent replications.

To examine the GMM, we follow the choice of the number of moment conditions used in Pei et al. (2025), and evaluate the joint pgf at a finite grid of points $(u, v) \in V \times V$, where

$$V = \{0.2,\ 0.4,\ 0.6,\ 0.8\}.$$

This choice yields $|V|^2 = 16$ moment conditions, which is sufficient to ensure parameter identification. The covariance matrix $\Omega(\theta)$ of the moment conditions can be computed explicitly. Pei et al. (2025) provide $\Omega(1,1)$ and $\Omega(1,2)$ elements, which are given by

$$\begin{aligned} \Omega_{11}(\theta) &= E_\theta \left(E_\theta \left[u_1^{X_t} v_1^{X_{t+1}} \right] - u_1^{X_t} v_1^{X_{t+1}} \right)^2 \\ &= E_\theta \left[u_1^{X_t} v_1^{X_{t+1}} \right] - \left(E_\theta \left[u_1^{X_t} v_1^{X_{t+1}} \right] \right)^2, \end{aligned} \tag{18}$$

$$\begin{aligned} \Omega_{12}(\theta) &= E_\theta \Big(E_\theta \left[u_1^{X_t} v_1^{X_{t+1}} \right] - u_1^{X_t} v_1^{X_{t+1}} \Big) \Big(E_\theta \left[u_1^{X_t} v_2^{X_{t+1}} \right] - u_1^{X_t} v_2^{X_{t+1}} \Big) \\ &= E_\theta \left[u_1^{X_t} (v_1 v_2)^{X_{t+1}} \right] - E_\theta \left[u_1^{X_t} v_1^{X_{t+1}} \right] E_\theta \left[u_1^{X_t} v_2^{X_{t+1}} \right], \end{aligned} \tag{19}$$

where $u_1 = 0.2$, $v_1 = 0.2$, and $v_2 = 0.4$.

For comparison, the maximum likelihood estimator of the pure causal and noncausal INAR(1) processes is also computed. It is based on formulas (14)-(15) with the same true parameter values.

The performance of the GMM and ML estimators is evaluated by calculating the finite sample bias and the standard deviation (SD) of the parameter estimates $\hat{\theta}_i$ of θ_i, $i = 1, ..., 4$ in the parameter vector $\theta = (\alpha, \beta, r, p)'$, across all replications $h = 1, ..., H$ using the following standard formulas:

$$\text{Bias}(\hat{\theta}_i) = \frac{1}{H}\sum_{h=1}^{H}(\hat{\theta}_{i,h} - \theta_{i,0}),\ i = 1, ..., 4 \tag{20}$$

$$\text{SD}(\hat{\theta}_i) = \sqrt{\frac{1}{H-1}\sum_{h=1}^{H}(\hat{\theta}_{i,h} - \bar{\hat{\theta}}_i)^2}\ i = 1, ..., 4 \tag{21}$$

where $\hat{\theta}_{i,h}$ is the parameter i^{th} estimate in the h^{th} replication, $\theta_{i,0}$ is the true value of parameter i, and $\bar{\hat{\theta}}_i$ is the average estimate across all H replications.

The performance of the MLE and GMM in application to the causal, noncausal and mixed integer autoregressive models is illustrated in Tables 2 and 3 respectively.

Table 2: Statistics summary of MLE for $\varepsilon_t \sim \text{NB}(r, p)$

Model	**Parameter**	**True**	T=1000		T=1500	
			Bias	SD	Bias	SD
Pure Causal	α	0.6	-0.0001	0.0091	-0.0011	0.0172
	r	0.05	0.0006	0.0047	0.0003	0.0084
	p	0.05	0.0021	0.0079	0.0030	0.0139
Pure Noncausal	β	0.6	0.0006	0.0093	0.0000	0.0163
	r	0.05	0.0002	0.0048	0.0009	0.00969
	p	0.05	0.0002	0.0069	0.0023	0.01503

Table 3: Statistics summary of GMM for $\varepsilon_t \sim \text{NB}(r, p)$

Model	**Parameter**	**True**	T=1000		T=2000	
			Bias	SD	Bias	SD
Pure Causal	α	0.6	0.0425	0.0098	0.0340	0.0880
	r	0.05	-0.0107	0.0065	0.0128	0.0690
	p	0.05	-0.0156	0.0158	0.0210	0.0140
Pure Noncausal	β	0.6	0.0429	0.0232	0.0380	0.0263
	r	0.05	-0.0119	0.0067	0.0126	0.0560
	p	0.05	-0.0170	0.0091	0.0210	0.0071
MIAR(1,1)	α	0.8	0.0046	0.0150	0.0023	0.0122
	β	0.2	0.0169	0.0610	0.0064	0.0350
	r	0.05	-0.0030	0.0101	0.0005	0.0071
	p	0.05	0.0015	0.0144	0.0018	0.0090

The results in Tables 2 and 3 indicate that the GMM exhibits poorer performance in the pure models, compared to the Maximum Likelihood estimator, with larger finite sample bias and standard deviations. The

GMM estimator performs relatively well in the mixed MIAR(1,1) model, for the large and well-chosen set of 16 moment conditions given above. The results given in Table 3 can be compared with those in Table 3 of Pei et al. (2025), page 347, where the same parameter values and the same moment conditions are considered. The sensitivity of the GMM estimator to the choice of moment conditions is illustrated in Table 5 of Pei et al. (2025), page 349, where the finite bias and standard deviations of GMM applied to the MIAR(1,1) model are compared across 3 different sets of moment conditions The Indirect Inference estimator introduced in the next Section does not require a judicious choice of moment conditions and provides estimators with even better finite sample properties.

4 Indirect Inference for INAR(1) Processes

This Section and the following one introduce Indirect Inference as an alternative estimation method for the noncausal and mixed count models, given that a) the performance of the GMM estimator revealed in the previous Section, and reported in Pei et al. (2025), Tables 3 and 5, is not always satisfactory and depends on the choice of moments, which is difficult in practice, and b) the ML estimator is not applicable to the MIAR(1,1) model. Below, we consider the Indirect Inference leading to plug-in estimators of causal and noncausal INAR(1) processes.

The Indirect Inference method exploits the relationship between the parameters of a model of interest and of an auxiliary model that is easier to estimate than the dynamic count model. Then, the parameters of the model of interest, such as the INAR(1) model with i.i.d. errors, can be inferred from the parameter estimates of the auxiliary model. The relationship between the parameters of the true and auxiliary models is represented by a binding function. Below, we discuss the binding functions for the pure causal and noncausal INAR(1) processes and the Gaussian AR(1) auxiliary model, and comment on the adequacy of the proposed auxiliary model.

4.1 Causal INAR(1) with Poisson errors and auxiliary Gaussian AR(1)

Let us consider as the DGP the causal INAR(1) model with $Z \sim \mathcal{B}(1, \alpha)$ and $\varepsilon \sim \mathcal{P}(\lambda)$. Then $X \sim \mathcal{P}(\frac{\lambda}{1-\alpha})$ (Gourieroux and Jasiak, 2004). The structural parameters are α, λ.

Let the auxiliary model be the Gaussian AR(1):

$$X_t = \phi X_{t-1} + \eta_t, \quad \text{where} \quad \eta_t \sim IIN(0, \sigma^2).$$

with auxiliary parameters ϕ and σ^2. We see that the DGP can be written as:

$$X_t = \alpha X_{t-1} + \varepsilon_t + \sum_{i=1}^{X_{t-1}} (Z_{i,t} - \alpha) = \alpha X_{t-1} + u_t,$$

where $u_t = \varepsilon_t + \sum_{i=1}^{X_{t-1}} (Z_{i,t} - \alpha)$ and $E(u_t|X_{t-1}) = 0$. The process (u_t) is a martingale difference sequence (MDS), but it is not a strong Gaussian white noise. Therefore the auxiliary model is misspecified.

The pseudo-maximum likelihood (PML) estimators $\hat{\phi}_T, \hat{\sigma}_T^2$ of ϕ, σ^2 based on T observations are consistent of the pseudo-true values $\phi_\infty, \sigma_\infty^2$:

$$\hat{\phi}_T \to \phi_\infty = \frac{Cov(X_t, X_{t-1})}{Var(X_{t-1})}, \quad \hat{\sigma}_T^2 \to \sigma_\infty^2 = Var(X_t)\,(1 - \phi_\infty^2).$$

We see that:

$$\phi_\infty = \alpha.$$

There is no asymptotic bias in the OLS estimation of α and

$$\sigma_\infty^2 = \frac{\lambda}{1-\alpha}(1-\alpha^2) = \lambda(1+\alpha).$$

Hence, the binding function is:

$$\begin{pmatrix} \alpha \\ \lambda \end{pmatrix} \overset{b(.)}{\to} \begin{pmatrix} \phi \\ \sigma^2 \end{pmatrix} = \begin{pmatrix} \alpha \\ \lambda(1+\alpha) \end{pmatrix}.$$

Its inverse is such that:

$$\alpha = \phi,\ \lambda = \frac{\sigma^2}{1+\phi},$$

or equivalently:

$$\begin{pmatrix} \phi \\ \sigma^2 \end{pmatrix} \overset{b(.)^{-1}}{\to} \begin{pmatrix} \alpha \\ \lambda \end{pmatrix} = \begin{pmatrix} \phi \\ \sigma^2/(1+\phi) \end{pmatrix}.$$

We observe that the binding function has a closed form. Hence, the true parameters can be obtained from a "plug-in" method as follows: first, we estimate the auxiliary model by OLS, which is asymptotically equivalent to the maximum likelihood based on a Gaussian log-likelihood function, to get $\hat{\phi}_T, \hat{\sigma}_T^2$. Next, the Indirect Inference estimates of the true parameters are: $\hat{\alpha}_{II,T} = \hat{\phi}_T$ and $\hat{\lambda}_{II,T} = \hat{\sigma}_T^2/(1+\hat{\phi}_T)$.

4.2 Noncausal INAR(1) with Poisson errors and auxiliary Gaussian AR(1)

Let us consider as the DGP the noncausal INAR(1) model with $Z \sim \mathcal{B}(1,\beta)$ and $\tilde{\varepsilon} \sim \mathcal{P}(\lambda)$. Then $X \sim \mathcal{P}(\frac{\lambda}{1-\beta})$. Let the auxiliary model be the Gaussian AR(1), as above. This choice of the auxiliary model is motivated by the fact that the OLS and the equivalent maximum likelihood based on a Gaussian log-likelihood function estimate consistently the autoregressive parameter in either the calendar or reverse time [Gourieroux and Jasiak (2018))]. Under the normality assumption on the error, the forward and backward dynamics cannot be distinguished, as the coefficients of the past and future errors in the moving average infinity representation of a Gaussian AR(1): $X_t = \sum_{i=-\infty}^{\infty} \phi^i \eta_{t-i}$ are identical.

The DGP can be written as:

$$X_t = \beta X_{t+1} + \tilde{\varepsilon}_t + \sum_{i=1}^{X_{t+1}} (Z_{i,t} - \beta) = \beta X_{t+1} + \tilde{u}_t$$

where $\tilde{u}_t = \tilde{\varepsilon}_t + \sum_{i=1}^{X_{t+1}} (Z_{i,t} - \beta)$ and $E(\tilde{u}_t | X_{t+1}) = 0$. Then, the process $(\tilde{u}_t)$ is a MDS in reversed time. As in the previous subsection, we see that the pseudo-true values are such that:

$$\phi_\infty = \beta.$$

There is no asymptotic bias in the OLS estimation of β and

$$\sigma_\infty^2 = \frac{\lambda}{1-\beta}(1-\beta^2) = \lambda(1+\beta).$$

Hence, the binding function is:

$$\begin{pmatrix} \beta \\ \lambda \end{pmatrix} \overset{b(.)}{\rightarrow} \begin{pmatrix} \phi \\ \sigma^2 \end{pmatrix} = \begin{pmatrix} \beta \\ \lambda(1+\beta) \end{pmatrix}.$$

Its inverse is such that:

$$\beta = \phi, \ \lambda = \frac{\sigma^2}{1+\phi},$$

$$\begin{pmatrix} \phi \\ \sigma^2 \end{pmatrix} \overset{b(.)^{-1}}{\rightarrow} \begin{pmatrix} \beta \\ \lambda \end{pmatrix} = \begin{pmatrix} \phi \\ \sigma^2/(1+\phi) \end{pmatrix}$$

It follows that a plug-in method can be applied to obtain the Indirect Inference estimates of the true model from the OLS or Gaussian maximum likelihood estimates $\hat{\phi}_T, \hat{\sigma}_T^2$ of the auxiliary model. The parameter estimates of the true parameters are: $\hat{\beta}_{II,T} = \hat{\phi}_T$ and $\hat{\lambda}_{II,T} = \hat{\sigma}_T^2/(1+\hat{\phi}_T)$.

Since the true model is a causal INAR(1) written in reversed time, and the Gaussian AR(1) model is time reversible, we observe that the binding functions (resp. their inverses) are the same in Examples 1 and 2. However, the plug-in approach is feasible only if we know a-priori whether the INAR(1) model is causal or noncausal. This is because the causal and noncausal dynamics cannot be identified in processes with Poisson distributed errors, as mentioned earlier in Section 3.3. Hence, the use of the above models is limited in practice, although the INAR(1) processes with Poisson distributed errors provide a convenient illustration of the Indirect Inference approach. Below, we consider pure causal and noncausal INAR(1) models with a Negative Binomial error distribution that ensures the identification of causal and noncausal dynamics and accommodates the unconditional overdispersion.

4.3 Noncausal INAR(1) with NB errors and auxiliary Gaussian AR(1)

Let us assume as the DGP a noncausal INAR(1) with the Negative Binomial $\mathcal{NB}(r,p)$ error distribution:

$$X_t = \sum_{i=1}^{X_{t+1}} Z_{i,t} + \tilde{\varepsilon}_t,$$

with $Z_{i,t} \sim \mathcal{B}(1,\beta)$ where $\beta \in (0,1)$, and i.i.d. errors $\tilde{\varepsilon}_t \sim \mathcal{NB}(r,p)$ where $r > 0$, $p \in (0,1)$. Then, the structural parameters are (β, r, p). The auxiliary Gaussian AR(1) model:

$$\begin{aligned} X_t &= \phi X_{t+1} + \eta_t, \text{ where } \eta_t \sim IIN(m, \sigma^2) \\ &= m + \phi X_{t-1} + v_t, \text{ where } v_t \sim IIN(0, \sigma^2) \end{aligned} \tag{22}$$

has 3 auxiliary parameters (m, ϕ, σ^2). The pseudo-true values $\phi_\infty, m_\infty, \sigma^2_\infty$ are such that:

$$\phi_\infty = \frac{Cov(X_t, X_{t-1})}{Var(X_{t-1})}, \quad m_\infty = EX_t(1-\phi_\infty) = EX_t\left(1 - \frac{Cov(X_t, X_{t-1})}{Var(X_{t-1})}\right),$$

$$\sigma^2_\infty = Var(X_t)\left[1 - \left(\frac{Cov(X_t, X_{t-1})}{Var(X_{t-1})}\right)^2\right] = Var(X_t)(1-\phi^2_\infty).$$

Proposition 1: For the INAR(1) with i.i.d. errors with $\mathcal{NB}(r,p)$ distribution, the binding function based on the auxiliary Gaussian AR(1) (with intercept) model (22) is one-to-one and such that:

$$\begin{pmatrix} \beta \\ r \\ p \end{pmatrix} \overset{b(.)}{\rightarrow} \begin{pmatrix} \phi \\ m \\ \sigma^2 \end{pmatrix} = \begin{pmatrix} \beta \\ r\frac{1-p}{p} \\ \frac{r(1-p)}{p}(\beta + \frac{1}{p}) \end{pmatrix}.$$

Proof:

The Noncausal INAR(1) process is :

$$X_t = \sum_{i=1}^{X_{t+1}} Z_{i,t} + \tilde{\varepsilon}_t,$$

where $Z_{i,t}$ are i.i.d with a $\mathcal{B}(1,\beta)$, and $\tilde{\varepsilon}_t$ are i.i.d with a mean denoted by μ and variance denoted by γ: $Var(\tilde{\varepsilon}_t) = \gamma$.

Let us compute the pseudo-true values $\phi_\infty, m_\infty, \sigma^2_\infty$ under this data generating process. The conditional expectation of the noncausal INAR(1) is:

$$E(X_t|X_{t+1}) = \beta X_{t+1} + \mu. \tag{23}$$

Let us introduce the projection $P[X_t|X_{t+1}]$ in L^2 of X_{t+1} on the set of linear affine functions of X_{t+1}. Since the conditional expectation $E(X_t|X_{t+1})$ is a projection on the set of nonlinear functions of X_{t+1}, we deduce from the Iterated Projection Theorem that:

$$P[E(X_t|X_{t+1})|X_{t+1}] = P[X_t|X_{t+1}].$$

Hence, $P[X_t|X_{t+1}] = \beta X_{t+1} + \mu$. It follows that:

$$\phi_\infty = \beta, \quad m_\infty = \mu.$$

Moreover, the conditional variance of the noncausal INAR(1) is:

$$Var(X_t|X_{t+1}) = \beta(1-\beta)X_{t+1} + \gamma.$$

Then, we deduce the marginal variance by applying the variance decomposition formula:

$$\begin{aligned} Var(X_t) &= VarE(X_t|X_{t+1}) + EVar(X_t|X_{t+1}) \\ &= Var(\beta X_{t+1} + \mu) + E[\beta(1-\beta)X_{t+1} + \gamma] \\ &= \beta^2 Var(X_{t+1}) + \beta(1-\beta)EX_{t+1} + \gamma. \end{aligned} \tag{24}$$

By the stationarity assumption, from (23) we get :

$$E(X_t) = \frac{\mu}{1-\beta},$$

and from (24):

$$Var(X_t) = \frac{1}{1-\beta^2}(\beta\mu + \gamma)$$

It follows that:

$$\sigma^2_\infty = \beta\mu + \gamma.$$

To summarize, we get a binding function linking the auxiliary parameters (ϕ, m, σ^2) with the structural parameters (β, μ, γ) as follows:

$$\begin{pmatrix} \phi \\ m \\ \sigma^2 \end{pmatrix} = \begin{pmatrix} \beta \\ \mu \\ \beta\mu + \gamma \end{pmatrix}$$

Let us now introduce the structural parameters corresponding to the negative binomial distribution. A Negative Binomial distribution is parametrized by n for the number of successes (r in the case of Polya distribution with a real-valued success number) and p for the probability of a success. It has the expected value $\mu = \frac{r(1-p)}{p}$ and variance $\gamma = \frac{r(1-p)}{p^2}$. In particular, the $\mathcal{NB}$ distribution allows for the overdispersion $\gamma \geq \mu$ often observed in practice. We observe that the mappings between the following parameters are:

$$\mu = r\frac{1-p}{p}, \quad \gamma = r\frac{1-p}{p^2},$$

which implies that:

$$\sigma^2_\infty = \beta\frac{r(1-p)}{p} + \frac{r(1-p)}{p^2} = \frac{r(1-p)}{p}\left[\beta + \frac{1}{p}\right].$$

Hence, the binding function linking (ϕ, m, σ^2) with (β, r, p) is:

$$\begin{pmatrix} \beta \\ r \\ p \end{pmatrix} \overset{b(.)}{\to} \begin{pmatrix} \phi \\ m \\ \sigma^2 \end{pmatrix} = \begin{pmatrix} \beta \\ r\frac{1-p}{p} \\ \frac{r(1-p)}{p}(\beta + \frac{1}{p}) \end{pmatrix}.$$

Let us now invert this binding function. Then we have $\frac{\sigma^2}{m} = \phi + \frac{1}{p} => \frac{\sigma^2 - \phi m}{m} = \frac{1}{p}$. Hence $p = \frac{m}{\sigma^2 - \phi m}$. Moreover, $\frac{1-p}{p} = \frac{1}{p} - 1 = \frac{\sigma^2 - (\phi+1)m}{m}$. Therefore $r = m\frac{p}{1-p} = \frac{m^2}{\sigma^2 - (\phi+1)m}$.

The inverse binding function is such that:

$$\begin{pmatrix} \phi \\ m \\ \sigma^2 \end{pmatrix} \overset{b(.)^{-1}}{\to} \begin{pmatrix} \beta \\ r \\ p \end{pmatrix} = \begin{pmatrix} \phi \\ m^2/(\sigma^2 - (\phi+1)m) \\ \frac{m}{\sigma^2 - \phi m} \end{pmatrix},$$

where $\sigma^2 - \phi m \neq 0$ because the equality $\sigma^2 = \phi m$ holds only when $1/p = 0$, i.e. $p = \infty$, which is excluded. In addition, $\sigma^2 \neq (\phi + 1)m$ by the same argument and the constraint $\beta \in (0, 1)$. The binding function has a closed form and the Indirect Inference estimates can be obtained by a plug-in method using the OLS or Gaussian maximum likelihood estimates as follows:

$$\hat{\beta}_{II,T} = \hat{\phi}_T, \quad \hat{p}_{II,T} = \frac{\hat{m}_T}{\hat{\sigma}^2_T - \hat{\phi}_T\hat{m}_T}, \quad \hat{r}_{II,T} = \hat{m}^2_T/(\hat{\sigma}^2_T - (\hat{\phi}_T + 1)\hat{m}_T).$$

5 Simulation-Based Indirect Inference for MIAR(1,1)

In this Section, we study the Indirect Inference for the mixed MIAR(1,1) model. The parameters of this model of interest are $\theta = (\alpha, \beta, r, p)$. Below, we discuss the binding function for the mixed MIAR(1,1) with i.i.d. Negative Binomial errors and an auxiliary Cauchy MAR(1,1) model which has the likelihood function in a closed form.

5.1 The DGP and the auxiliary model

We consider as the data generating process the MIAR(1,1) model in eq.(12):

$$X_t = [u_t + \varepsilon_t] + v_{t+1} \equiv [\varepsilon_t + v_{t+1}] + u_t,$$

with $\varepsilon_t \sim \mathcal{NB}(r,p)$ with $r>0, p \in (0,1)$ and u_t, v_t respectively are the (thinned) causal and noncausal components. The parameters of this model are: α, β, r, p, where $\alpha \in (0,1)$ and $\beta \in (0,1)$ are the thinning parameters, and we can write:

$$\begin{aligned} X_t &= \varepsilon_t + \sum_{k=1}^{\infty} \varepsilon_{t-k}(t) + \sum_{k=1}^{\infty} \varepsilon_{t+k}(t) \\ &= \varepsilon_t + u_t + v_{t+1}, \end{aligned}$$

where the $\varepsilon_{t-k}(t)$ and $\varepsilon_{t+k}(t)$ satisfy the recursive formulas given in Pei et al. (2025):

$$\varepsilon_s(t+1) = \sum_{i=1}^{\varepsilon_s(t)} Z_{i,s,t}, \quad t \geq s, \quad \text{with } \varepsilon_s(s) = \varepsilon_s$$

$$\varepsilon_t(s-1) = \sum_{j=1}^{\varepsilon_t(s)} Z^*_{ij,s,t}, \quad s \leq t, \quad \text{with } \varepsilon_s(s) = \varepsilon_s$$

where $Z_{i,s,t}$ (resp. $Z^*_{j,s,t}$) are i.i.d. accross $i,s,t(j,s,t)$ and are Bernoulli(α) (resp. Bernoulli(β)) distributed. Suppose $\varepsilon_t \sim \mathcal{NB}(r,p)$, $\alpha_0 \in [0,1), \beta_0 \in [0,1)$. The above expression can be interpreted as the causal INAR: $u_t + \varepsilon_t$ plus v_{t+1}, or the noncausal INAR: $v_{t+1} + \varepsilon_t$ plus u_t, otherwise the error term ε_t would be counted twice. From Section 2.3 of Pei et al. (2025), it follows that for the causal part:

$$E[\varepsilon_s(s+k)|\varepsilon] = \alpha^k \varepsilon_s = E[\varepsilon_s(s+k)|\varepsilon_s],$$

where $\varepsilon = (\varepsilon_s)$ includes the past, present and future values of ϵ. Hence, under conditional expectation, the true MA representation in ε of the causal part including the error term becomes:

$$E(u_t|\varepsilon) + \varepsilon_t = \varepsilon_t + \alpha\varepsilon_{t-1} + \alpha^2\varepsilon_{t-2} + \cdots \tag{25}$$

For the noncausal part, we have similarly [see Section 2.3 of Pei et al. (2025)]:

$$E[\varepsilon_s(s-k)|\varepsilon] = \beta^k \varepsilon_s = E[\varepsilon_s(s-k)|\varepsilon_s].$$

Hence, under conditional expectation, the MA representation in ε of the noncausal part becomes:

$$E(v_{t+1}|\varepsilon) = \beta\varepsilon_{t+1} + \beta^2\varepsilon_{t+2} + \beta^3\varepsilon_{t+3} + \cdots \tag{26}$$

Then, we deduce that the process of conditional expectation $X^*_t = E(X_t|\epsilon)$ is such that:

$$X^*_t = \sum_{j=0}^{\infty} \alpha^j \varepsilon_{t-j} + \sum_{j=1}^{\infty} \beta^j \varepsilon_{t+j},$$

or, equivalently, the (latent) process (X^*_t) is stationary and satisfies the causal-noncausal model:

$$(1 - \alpha L)(1 - \beta L^{-1})X_t^* = \varepsilon_t.$$

This explains the choice of the MAR(1,1) as the auxiliary model with a similar dynamic structure, but written in X_t instead of X_t^*, hence misspecified. The Mixed Autoregressive MAR(1,1) process used as the auxiliary model is:

$$(1 - \phi L)(1 - \psi L^{-1})X_t = e_t, \tag{27}$$

where $e_t = m + \sigma\eta_t$, e_t (resp. η_t) is i.i.d. non Gaussian with location m and scale σ (resp. with location 0 and unitary scale), and $\phi, \psi \in (0, 1)$. For example, the error distribution can be Cauchy, or t-student. In the former case, the auxiliary parameters are $\delta = (\phi, \psi, m, \sigma)$. Because we replace X_t^* by X_t, we cannot expect ex-ante that the pseudo auxiliary parameters ϕ, ψ coincide with α, β.

5.2 Approximate Maximum Likelihood

The MAR(1,1) is a special case of a more general mixed (causal-noncausal) autoregressive process $\{y_t; t = 0, \pm1, \pm2, ...\}$, defined in a multiplicative form as:

$$\Phi(L)\Psi(L^{-1})y_t = e_t,$$

where $\Psi(L^{-1})$ and $\Phi(L)$ are finite order polynomials in the negative (resp. positive) powers of the lag operator L. The polynomials are such that $\Psi(0) = \Psi(0) = 1$ and their roots are assumed to lie outside the unit circle. The error terms e_t are identically and independently distributed (i.i.d.). Under the above assumptions, $\{y_t\}$ has a unique stationary solution, which admits a strong, two-sided moving average representation in past and future errors. As mentioned earlier, under the normality assumption on the error, the forward and backward dynamics cannot be distinguished, as the coefficients of the past and future errors in the moving average infinity representation of a Gaussian MAR(1,1) are identical. However, the autoregressive parameters ϕ, ψ of the MAR(1,1) model are identifiable as long as the error term is not Gaussian[2]. For example, Lanne and Saikkonen (2011) consider the t-Student distributed errors, while Gouriéroux and Zakoïan (2017) introduce the Cauchy distributed errors, characterized by a heavy-tailed marginal density function. Then, model (27) with errors $\eta_t \sim Cauchy(0, 1)$ is a mixed autoregressive MAR(1,1) model with Cauchy distributed errors.

The auxiliary parameter $\delta = (m, \sigma, \phi, \psi)$ can be estimated by the Approximate Maximum Likelihood (AML) [see, Breidt et al. (), Lanne and Saikkonen (2011), Section 3.1] valid under the multiplicative form. The approximate log-likelihood function with $\delta = (m, \sigma, \phi, \psi)$:

$$\log L_T(\delta) = \sum_{t=2}^{T-1} \log\left(\frac{1}{\pi\sigma}\frac{1}{1 + [\frac{1}{\sigma}(-\phi X_{t-1} + (1 + \phi\psi)X_t - \psi X_{t+1} - m)]^2}\right),$$

[2]See e.g. Cheng (1992), Rosenblatt (2000), Theorem 1.3.1. for errors with finite variance, Breidt, Davis (1992) for errors with finite expectation and infinite variance, Gourieroux, Zakoian (2013)b for errors without finite expectation, as the Cauchy errors considered in the application.

is interpreted as the pseudo-log likelihood function. When $T \to \infty$, we get the asymptotic pseudo log-likelihood:

$$
\begin{aligned}
L_\infty(\delta,\theta) &:= lim_{T\to\infty}\frac{1}{T}\log L_T(\delta,\theta) \\
&= -\log\pi + E_\theta\left[-\log\sigma - \log[1+\left(\frac{1}{\sigma}(-\phi X_{t-1}+(1+\phi\psi)X_t-\psi X_{t+1}-m)\right)^2]\right], \qquad (28)
\end{aligned}
$$

where E_θ denotes the expectation with respect to the DGP evaluated at the value θ of the structural parameter. The pseudo-true values $m_\infty, \sigma_\infty, \phi_\infty, \psi_\infty$ are the arguments that maximize the above asymptotic expression.

The first-order conditions (FOC) are:

$$
\frac{\partial \log L_T(\delta,\theta)}{\partial\phi} = 0 \iff
$$

$$
E_\theta\left\{[-\frac{2}{\sigma}(-X_{t-1}+\psi X_t)(-\phi X_{t-1}+(1+\phi\psi)X_t-\psi X_{t+1}-m)]/[1+\left(\frac{1}{\sigma}(-\phi X_{t-1}+(1+\phi\psi)X_t-\psi X_{t+1}-m)\right)^2]\right\}=0
$$

$$
\frac{\partial \log L_T(\delta,\theta)}{\partial\psi} = 0 \iff
$$

$$
E_\theta\left\{[-\frac{2}{\sigma}(-X_{t+1}+\phi X_t)(-\phi X_{t-1}+(1+\phi\psi)X_t-\psi X_{t+1}-m)]/[1+\left(\frac{1}{\sigma}(-\phi X_{t-1}+(1+\phi\psi)X_t-\psi X_{t+1}-m)\right)^2]\right\}=0
$$

$$
\frac{\partial \log L_T(\delta,\theta)}{\partial m} = 0 \iff
$$

$$
E_\theta\left\{[\frac{2}{\sigma}(-\phi X_{t-1}+(1+\phi\psi)X_t-\psi X_{t+1}-m)]/[1+\left(\frac{1}{\sigma}(-\phi X_{t-1}+(1+\phi\psi)X_t-\psi X_{t+1}-m)\right)^2]\right\}=0
$$

$$
\frac{\partial \log L_T(\delta,\theta)}{\partial\sigma} = 0 \iff
$$

$$
E_\theta\left\{-\frac{1}{\sigma}+[\frac{2}{\sigma^3}(-\phi X_{t-1}+(1+\phi\psi)X_t-\psi X_{t+1}-m)^2]/[1+\left(\frac{1}{\sigma}(-\phi X_{t-1}+(1+\phi\psi)X_t-\psi X_{t+1}-m)\right)^2]\right\}=0
$$

The first-order conditions with respect to m and σ are difficult to compute. Therefore, the analytical formula of the binding function is not derived.

5.3 Approximate binding function

However, we can approximate the pseudo-true values of the auxiliary parameters. The above FOC are weighted covariance conditions with stochastic weights: $1/[1+\left(\frac{1}{\sigma}(-\phi X_{t-1}+(1+\phi\psi)X_t-\psi X_{t+1}-m)\right)^2]$, which are strictly stationary under the DGP. Let us now approximate the FOC by their unweighted expectations under the DGP, i.e. with the stochastic weights replaced by their expectations. Then, the approximate three first FOCs written using a different parameterization in $(\phi, \psi, \mu = [m/(1-\phi)(1-\psi)], \sigma)$ lead to:

$$
E_\theta\left([-(X_{t-1}-\mu)+\psi(X_t-\mu)][-\phi(X_{t-1}-\mu)+(1+\phi\psi)(X_t-\mu)+\psi(X_{t+1}-\mu)]\right)=0,
$$

$$
E_\theta\left([-(X_{t+1}-\mu)+\phi(X_t-\mu)][-\phi(X_{t-1}-\mu)+(1+\phi\psi)(X_t-\mu)+\psi(X_{t+1}-\mu)]\right)=0,
$$

$$E_\theta[-\phi(X_{t-1}-\mu)+(1+\phi\psi)(X_t-\mu)-\psi(X_{t+1}-\mu)]=0,$$

It is easy to see that the solution of this system is:

$$\tilde{\mu}_\infty = E_\theta(X_t), \tilde{\phi}_\infty = \alpha, \tilde{\psi}_\infty = \beta$$

since the first two FOC's can be interpreted as the orthogonality conditions of the latent non-causal and causal components v_{t-1} and u_{t+1}, respectively, and ε_t [see Gourieroux and Jasiak (2023)]. Therefore, we can expect that the true pseudo-true values $\mu_\infty, \phi_\infty, \psi_\infty$ are close to these approximated values. From these results, it follows that:

Proposition 2: For the MIAR(1,1) with i.i.d. errors with a $\mathcal{NB}(r,p)$ distribution, the approximate binding function based on the auxiliary Cauchy MAR(1,1) model with location μ and error scale σ is such that $\tilde{\mu}_\infty = E_\theta(X_t), \tilde{\phi}_\infty = \alpha, \tilde{\psi}_\infty = \beta$.

Then, the fourth FOC evaluated at μ, α, β becomes:

$$\begin{aligned} - & \frac{1}{\sigma} E_\theta\left[1+\frac{1}{\sigma}[-\alpha(X_{t-1}-\mu)+(1+\alpha\beta)(X_t-\mu)-\beta(X_{t+1}-\mu)]^2\right] \\ + & \frac{2}{\sigma^2} E_\theta[(-\alpha(X_{t-1}-\mu)+(1+\alpha\beta)(X_t-\mu)-\beta(X_{t+1}-\mu)]^2 = 0 \end{aligned}$$

5.4 The Indirect Inference Algorithm

Without the above approximation, we can apply the simulation-based Indirect Inference approach. Then, under the Indirect Inference [Gourieroux et al. (1993)] the structural count model needs to be simulated and next the parameters $\theta = (\alpha, \beta, r, p)$ of the MIAR(1,1) with errors that follow a $\mathcal{NB}(p,r)$ distribution, for example, can be calibrated using the approximate maximum likelihood estimates obtained from the auxiliary MAR(1,1) model.

The Indirect Inference estimator $\hat{\theta}_{II}$ is obtained from the following steps:

1. Estimate the parameters $\hat{\delta}_T$ of the auxiliary model from the observed data $\{X_t\}_{t=1}^T$.
2. For a given parameter θ of the data generating process (DGP), generate H simulated paths of the MIAR(1,1) process to obtain $\{\hat{X}_t^h(\theta), t=1,...,T\}_{h=1}^H$.
3. Estimate the auxiliary parameters $\tilde{\delta}_{T,h}(\theta)$, $h=1,...,H$, from each simulated path.
4. The Indirect Inference estimator minimizes the distance between the parameter estimates of the auxiliary model based on the observed and simulated realizations:

$$\hat{\theta}_{II,H,T} = \arg\min_\theta \left[\hat{\delta}_T - \frac{1}{H}\sum_{h=1}^H \tilde{\delta}_{T,h}(\theta)\right]' W \left[\hat{\delta}_T - \frac{1}{H}\sum_{h=1}^H \tilde{\delta}_{T,h}(\theta)\right].$$

where W is a positive-definite weighting matrix.

Under this approach, it is necessary to simulate H times for each value of θ involved in the minimization algorithm. As mentioned in Gourieroux et al. (1993), this is equivalent to generating TH values of the simulated variables $\hat{X}_t(\theta), t = 1, ..., TH$ in a single path and estimating once $\tilde{\delta}_{TH}(\theta)$. Then, the Indirect Inference estimator minimizes the following objective function:

$$\hat{\theta}_{II,HT} = \arg\min_{\theta} \left[\hat{\delta}_T - \tilde{\delta}_{TH}(\theta)\right]' W \left[\hat{\delta}_T - \tilde{\delta}_{TH}(\theta)\right], \tag{29}$$

In the case of a just identified system, when the number of parameters in the models of interest and auxiliary are equal, the weighting matrix W can be replaced by an identity matrix, without loss of generality.

The asymptotic properties of the Indirect Inference estimators are simplified in the just-identified models $dim(\theta) = dim(\delta)$. Let us consider the estimators $\hat{\delta}_T$ and $\hat{\theta}_T$ based on samples of T observations. It follows from Gouriéroux and Monfort (1996), Property 4.2, that under the standard regularity conditions when $T \to \infty$, we have the following:

i) The Indirect Inference estimator $\hat{\theta}_{HT}$ is consistent, asymptotically normal when H is fixed and T tends to infinity:

$$\sqrt{T}(\hat{\theta}_{HT} - \theta_0) \xrightarrow{d} N(0, (1 + \tfrac{1}{H}) \left\{ \frac{\partial \delta'(\theta_0)}{\partial \theta} J_0 I_0^{-1} J_0 \frac{\partial \delta(\theta_0)}{\partial \theta'} \right\}^{-1})$$

where for the criterion function $K_T(\delta) = \frac{1}{T} logL_T(\delta)$ based on the log-likelihood of an auxiliary model, which converges to $L_\infty(\theta)$, we have:

$$J_0 = plim_T - \frac{\partial^2 K_T(\delta(\theta_0))}{\partial \delta \partial \delta'}$$

$$I_0 = \lim_T Var_0 \left\{ \sqrt{T} \tfrac{\partial K_T(\delta(\theta_0))}{\partial \delta} - E_0 \left(\sqrt{T} \tfrac{\partial K_T(\delta(\theta_0))}{\partial \delta} \right) \right\}.$$

The above matrices can be estimated knowing that:

$$J(\theta) = plim_T - \tfrac{1}{T} \textstyle\sum_{t=1}^T \frac{\partial^2 logf(x_t; \delta(\theta))}{\partial \delta \partial \delta'} = -E_\theta \left[\frac{\partial^2 logf(X_t; \delta(\theta))}{\partial \delta \partial \delta'} \right]$$

$$I(\theta) = lim_T Var_\theta \left\{ \tfrac{1}{\sqrt{T}} \textstyle\sum_{t=1}^T \left[\tfrac{\partial logf(x_t;\delta(\theta))}{\partial \delta} - E_\theta \left(\tfrac{\partial logf(X_t;\delta(\theta))}{\partial \delta} \right) \right] \right\}.$$

and $logf(x_t; \delta(\theta))$ is the log-likelihood of the auxiliary model at time t.

5.5 Covariance Estimator

Let $\{X_t, t = 1, ..., T\}$ follow the MIAR(1,1) model with the unknown parameter vector $\theta^* = (\mu, \sigma, \alpha, \beta)$. The discussion in Section 5.3 suggests an alternative estimator, which exploits the approximate zero covariance conditions for the latent causal and non-causal components and errors of the auxiliary model that is easier to estimate than the MIAR(1,1) model. We consider the following theoretical covariances and error moments:

$$s(\theta_0^*, \theta^*) = \begin{cases} E_{\theta_0^*}(e_t) = 0 \iff E_{\theta_0^*}[(1 - \alpha L)(1 - \beta L^{-1})(X_t - \mu)] = 0, \\ Cov_{\theta_0^*}(u_{t+1}, e_t) = 0 \iff Cov_{\theta_0^*}\{[-(X_{t+1} - \mu) + \alpha(X_t - \mu)], [(1 - \alpha L)(1 - \beta L^{-1})(X_t - \mu)]\} = 0, \\ Cov_{\theta_0^*}(v_{t-1}, e_t) = 0 \iff Cov_{\theta_0^*}\{[-(X_{t-1} - \mu) + \beta(X_t - \mu)], [(1 - \alpha L)(1 - \beta L^{-1})(X_t - \mu)]\} = 0, \\ E_{\theta_0^*}(e_t^2) = \sigma^2 \iff E_{\theta_0^*}[(1 - \alpha L)(1 - \beta L^{-1})(X_t - \mu)]^2 - \sigma^2 = 0, \end{cases}$$

where $(1-\alpha L)(1-\beta L^{-1})(X_t-\mu)=e_t, -(X_{t-1}-\mu)+\beta(X_t-\mu)=v_{t-1}, -(X_{t+1}-\mu)+\alpha(X_t-\mu)=u_{t+1}$ are the errors and latent non-causal and causal components, respectively. These quantities are matched with their empirical counterparts:

$$\hat{s}_T(\theta^*) = \begin{cases} \frac{1}{T}\sum_{t=2}^{T-1}\hat{e}_t(\theta^*)=0, \\ \frac{1}{T}\sum_{t=2}^{T-1}\hat{u}_{t+1}(\theta^*)\hat{e}_t(\theta^*) - \frac{1}{T}\sum_{t=2}^{T-1}\hat{u}_{t+1}(\theta^*)\frac{1}{T}\sum_{t=2}^{T-1}\hat{e}_t(\theta^*)=0 \\ \frac{1}{T}\sum_{t=2}^{T-1}\hat{v}_{t-1}(\theta^*)\hat{e}_t(\theta^*) - \frac{1}{T}\sum_{t=2}^{T-1}\hat{v}_{t+1}(\theta^*)\frac{1}{T}\sum_{t=2}^{T-1}\hat{e}_t(\theta^*)=0 \\ \frac{1}{T}\sum_{t=2}^{T-1}\hat{e}_t^2(\theta^*)-\sigma^2=0 \end{cases}$$

where $\hat{\varepsilon}_t(\theta^*), \hat{u}_t(\theta^*), \hat{v}_t(\theta^*)$ are the empirical counterparts of the errors and latent causal and non-causal components, respectively. The conditions involve a nonlinear function of X_t to ensure the identification of the forward-looking dynamics [Cite Chan here] and produce estimator $\hat{\theta^*}=(\hat{\mu},\hat{\sigma},\hat{\alpha},\hat{\beta})$. This estimator belongs in the class of GCov estimators [Gourieroux, Jasiak (2017),(2023)] but is not optimally weighted.

6 Indirect Inference - Simulation and Empirical Application

In this Section, we study the performance of the proposed inference estimator and apply them to the count variables of sentiment.

6.1 Indirect Inference - Simulation Study

We study the performance of the Indirect Inference methods and compare it with the estimators proposed in the existing literature.

Let us consider a MIAR(1,1) process (eq.12) with i.i.d. innovations following a negative binomial distribution. This process is generated in samples of length T = 500 and 1000 using the simulation algorithm given in Section 3.6. We consider three different sets of true parameters used in Pei et al. (2025). In the first experiment we consider parameter set 1 with $\alpha = 0.8$ and $\beta = 0.2$, and r and p equal to 0.05. The parameter sets 2 and 3 differ in terms of parameters α and β equal to $\{0.5, 0.5\}$ and $\{0.2, 0.8\}$, respectively. The number of replications is 100 in all experiments, similar to Pei et al. (2025).

For each set of parameter values, we simulate the series for t= 1,.., T=800,and discard the first 250 and last 50 realizations. Figure 3a shows this simulated path of T=500 obtained from the first set of parameters and Figure 3b shows its autocorrelation function. This simulated series has mean 5 and variance 40 and displays explosive patterns.

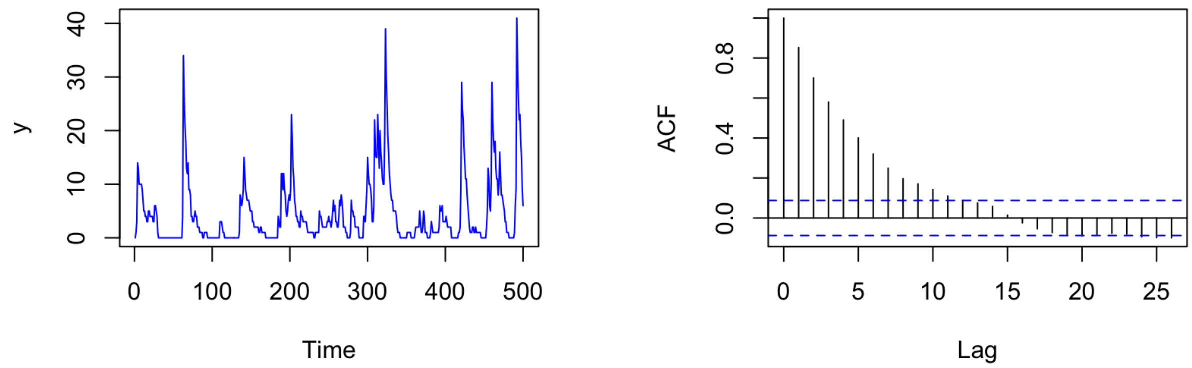

(a) Simulated Y_t

(b) Autocorrelation function of Y_t

Figure 3: Simulation of set 1, N=500 and its ACF

After generating the MIAR(1,1) processes using the three sets of parameter values and negative binomial errors, we use these simulated series as our "observed data" and estimate the MIAR(1,1) models by the Indirect Inference estimator. The auxiliary model considered is the MAR(1,1) process with location μ and Cauchy distributed errors with scale σ. The auxiliary parameters are estimated by the maximum likelihood, which is computed by the L-BFGS-B algorithm in R. The Indirect Inference estimator of the MIAR(1) model minimizes the distance between the auxiliary parameter estimates based on the observed and simulated data given in eq. (29).

The results are reported in Table 4 for three different sets of parameter values given above and considered in Pei et al. (2025). We observe that as the sample size increases to T=1000, the finite sample bias and SD of the Indirect Inference estimator decrease.

Table 4: Indirect Inference: MIAR(1,1) with $\varepsilon_t \sim \text{NB}(n, p)$

Model	**Parameter**	**True**	T=500		T=1000	
			Bias	SD	Bias	SD
Parameter-set 1	α	0.8	0.0030	0.0209	-0.0000	0.0012
	β	0.2	-0.0032	0.0221	0.0002	0.0012
	r	0.05	0.0005	0.0067	0.0013	0.0034
	p	0.05	0.0001	0.0058	0.0005	0.0027
Parameter-set 2	α	0.5	-0.0004	0.0188	-0.0003	0.0026
	β	0.5	-0.0017	0.0189	0.0002	0.0023
	r	0.05	0.0004	0.0046	0.0007	0.0027
	p	0.05	0.0021	0.0068	0.0008	0.0030
Parameter- set 3	α	0.2	0.0009	0.0260	-0.0004	0.0101
	β	0.8	0.0016	0.0221	-0.0005	0.0100
	r	0.05	0.0005	0.0057	0.0008	0.0037
	p	0.05	0.0006	0.0061	0.0005	0.0038

We can compare these results with the performance of GMM estimators reported in Pei et al. (2025) and given in Tables 3 and 5, Sections 5.3 and 5.4, respectively. The finite sample bias and SD of the Indirect Inference estimator are smaller than those of the GMM estimator reported in Pei et al. (2025). They are also smaller than the bias and SD of the GMM estimator of MIAR(1,1) reported in Table 3, Section 3.6, and obtained from the moment conditions used in Pei et al. (2025) for the first set of parameter values. We observe that for all parameter values and sample sizes considered, the Indirect Inference estimator has lower finite sample bias and smaller standard deviation by at least a factor 10.

6.2 Application to Tweet Counts

The MIAR(1,1) model is fitted to the series of negative tweets on AAPL and GME stocks of length T=285 and 435, respectively, as described in Section 2. We assume that the errors ε_t's follow the negative binomial distribution. We apply the Indirect Inference method and use the MAR(1,1) with Cauchy distributed errors as an auxiliary model to estimate the parameters of the MIAR(1,1) model.

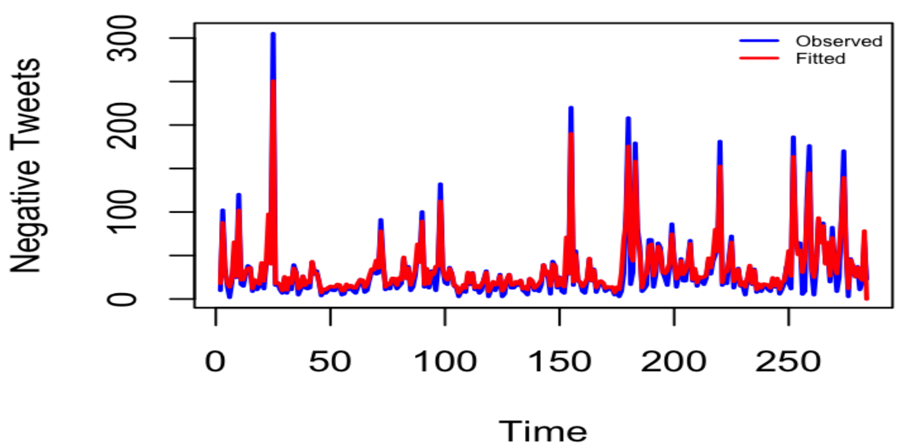

Figure 4: MIAR(1,1) fitted values- AAPL

The parameter estimates of the Indirect Inference for tweet counts on AAPLE and GME stocks are reported in Table 5. The standard error calculation for the Indirect Inference is based on the asymptotic variance matrix of the estimator given in Section 5.4.

Table 5: Estimation of MIAR(1,1) Model- AAPL

	Indirect Inference:AAPL			Indirect Inference:GME		
Parameter	Estimate	Std. Error	t-ratio	Estimate	Std. Error	t-ratio
α	0.799	0.029	27.40	0.907	0.0204	44.46
β	0.200	0.017	11.21	0.109	0.0447	2.438
r	0.120	0.013	8.64	0.243	0.0117	20.769
p	0.089	0.004	20.12	0.023	0.0255	0.901

The in-sample fitted values of the MIAR model are shown in Figures 4 and 5 for AAPL and GME tweet counts.

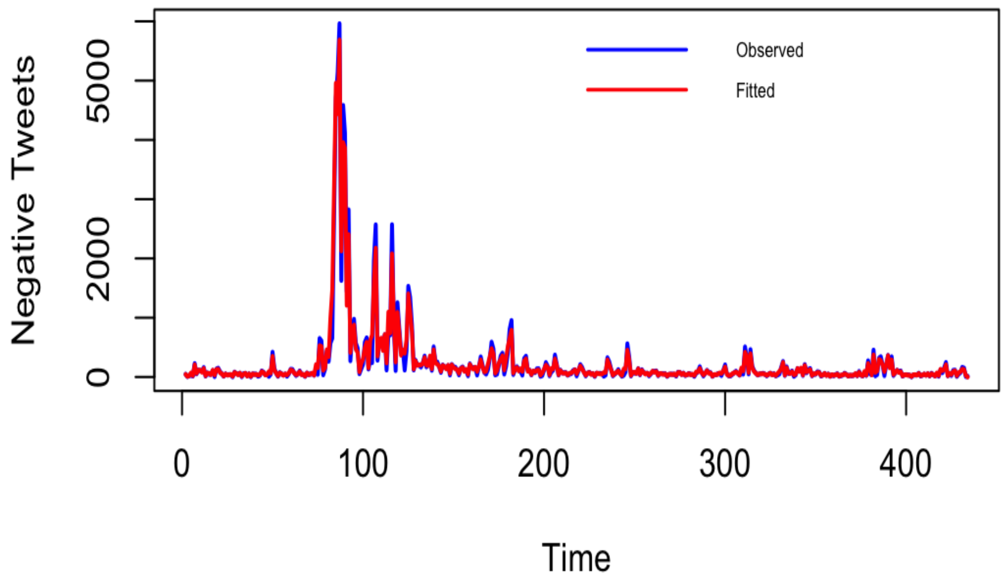

Figure 5: MIAR(1,1) fitted values- GME

7 Conclusion

We introduced the Indirect Inference estimation method for integer data with locally explosive patterns. The estimator performs well in simulations and in the application to sentiment data.

References

Al-Osh, M. A. and Alzaid, A. A. (1987). First-order integer-valued autoregressive (inar(1)) process. *Journal of Time Series Analysis*, 8(3):261–275.

Alzaid, A. A. and Al-Osh, M. (1990). An integer-valued pth-order autoregressive structure (inar(p)) process. *Journal of Applied Probability*, 27(2):314–324.

Foster, J. H. and Williamson, J. A. (1971). Limit theorems for the Galton-Watson process with time-dependent immigration. *Probability Theory and Related Fields*, 20(3):227–235.

Gourieroux, C. and Jasiak, J. (2004). Heterogeneous inar(1) model with application to car insurance. *Insurance: Mathematics and Economics*, 34(2):177–192.

Gourieroux, C. and Jasiak, J. (2018). Misspecification of noncausal order in autoregressive processes. *Journal of Econometrics*, 205(1):226–248.

Gourieroux, C. and Jasiak, J. (2023). Generalized covariance estimator. *Journal of Business & Economic Statistics*, 41(4):1315–1327.

Gourieroux, C., Monfort, A., and Renault, E. (1993). Indirect inference. *Journal of Applied Econometrics*, 8(S):S85–118.

Gouriéroux, C. and Lu, Y. (2021). Noncausal counting processes: A queuing perspective. *Electronic Journal of Statistics*, 15(2):3852–3891.

Gouriéroux, C. and Monfort, A. (1996). *Simulation-based Econometric Methods*. CORE Lectures. Oxford University Press, Oxford, UK.

Gouriéroux, C. and Zakoïan, J.-M. (2017). Local explosion modelling by non-causal process. *Journal of the Royal Statistical Society Series B (Statistical Methodology)*, 79(3):737–756.

Lanne, M. and Saikkonen, P. (2011). Noncausal autoregressions for economic time series. *Journal of Time Series Econometrics*, 3(3):1–32.

McKenzie, E. (1985). Some simple models for discrete variate time series. *Journal of The American Water Resources Association*, 21(4):645–650.

Pei, J., Lu, Y., and Zhu, F. (2025). Mixed causal-noncausal count process. *TEST: An Official Journal of the Spanish Society of Statistics and Operations Research*, 34(2):325–360.

Appendix

A.1 Two-Sided Moving Average (MA) Representations

The two-sided moving average (MA) representations depend on the underlying error terms and their properties, e.g. if the errors satisfy the strong or weak white noise conditions, and on the type of relationships between the observed time series and these white noises, which can be linear or nonlinear. Two types of MA representations have been considered in the paper and are compared below.

i) **The strong nonlinear MA representation**

The MA representations used to define the DGP are two-sided nonlinear moving averages based on noises (ε_t) and $(Z_{j,t})$. The nonlinearity is created by the thinning operator which is stochastic in Z. The process is initially defined by a nonlinear autoregressive equation that can be solved to deduce the associated two-sided moving average.

a) INAR (1) causal

$$X_t = B_t(\alpha) \circ X_{t-1} + \varepsilon_t \text{ with the thinning operator } B_t(\alpha) \circ X_{t-1} = \sum_{j=1}^{X_{t-1}} Z_{j,t}, \quad Z_{j,t} \; iid \; \mathcal{B}(1,\alpha)$$

The MA representation in (ε, Z) is:

$$\begin{aligned} X_t &= \varepsilon_t + B_t(\alpha) \circ [B_{t-1}(\alpha) \circ X_{t-2} + \varepsilon_{t-1}] \\ &= \varepsilon_t + B_{t,2}(\alpha) \circ B_{t-1}(\alpha) \circ X_{t-2} + B_{t,1}(\alpha) \circ \varepsilon_{t-1} \\ &= \varepsilon_t + B_{t,1}(\alpha) \circ \varepsilon_{t-1} + B_{t,2}(\alpha) \circ B_{t-1,1}(\alpha) \circ \varepsilon_{t-2} \\ &+ \cdots + B_{t,h}(\alpha) \circ B_{t-1,h-1}(\alpha) \circ \cdots \circ B_{t-h+1,1}(\alpha) \circ \varepsilon_{t-h}, \end{aligned}$$

which is written as:

$$\begin{aligned} X_t &= \varepsilon_t + \sum_{k=1}^{\infty} \varepsilon_{t-k}(t) \\ &= \varepsilon_t + \varepsilon_{t-1}(t) + \varepsilon_{t-2}(t) + \cdots + \varepsilon_{t-k}(t) + \cdots \end{aligned}$$

b) INAR(1) noncausal

The nonlinear stochastic noncausal autoregression is:

$$X_t = B_t(\beta) \circ X_{t+1} + \varepsilon_t \text{ with } B_t(\beta) \circ X_{t+1} = \sum_{i=1}^{X_{t+1}} Z_{i,t}, \quad Z_{j,t} \; iid \; \mathcal{B}(1,\beta)$$

The MA representation in (ε, Z) is:

$$\begin{aligned} X_t &= \varepsilon_t + B_t(\beta) \circ [B_{t+1}(\beta) \circ X_{t+2} + \varepsilon_{t+1}] \\ &= \varepsilon_t + B_{t,2}(\beta) \circ B_{t+1}(\beta) \circ X_{t+2} + B_{t,1}(\beta) \circ \epsilon_{t+1} \\ &= \varepsilon_t + B_{t,1}(\beta) \circ \varepsilon_{t+1} + B_{t,2}(\beta) \circ B_{t+1,1}(\beta) \circ \varepsilon_{t+2} \\ &+ \cdots + B_{t,h}(\beta) \circ B_{t+1,h-1}(\beta) \circ \cdots \circ B_{t+h+1,1}(\alpha) \circ \varepsilon_{t+h} \end{aligned}$$

This can be written as:

$$X_t = \varepsilon_t + \varepsilon_{t+1}(t) + \varepsilon_{t+2}(t) + \cdots + \varepsilon_{t+k}(t) + \cdots$$

c) MIAR(1,1)

Similarly, we can write:

$$X_t = \varepsilon_t + \sum_{k=1}^{\infty} \varepsilon_{t-k}(t) + \sum_{k=1}^{\infty} \varepsilon_{t+k}(t) \tag{a.1}$$
$$= \varepsilon_t + u_t + v_{t+1},$$

ii) **Weak two-sided MA representation**

We have shown in Section 5 that the MIAR(1,1) process is such that:

$$(1-\alpha L)(1-\beta L^{-1})X_t^* = \varepsilon_t \tag{a.2}$$

with $X_t^* = E(X_t|\varepsilon)$.

We will focus on this mixed framework since the INAR(1) processes correspond to the special cases $\alpha = 0$ or $\beta = 0$.

Equivalently, we have:

$$(1-\alpha L)(1-\beta L^{-1})(X_t^* - e_t^*) = \varepsilon_t, \tag{a.3}$$

where $e_t = X_t - X_t^*$ is the prediction error given ε.

Let us denote by:

$$X_t^* = c(L)\varepsilon_t = \sum_{j=-\infty}^{\infty} c_j \varepsilon_{t+j}, \tag{a.4}$$

the two-sided linear MA representation of X_t^* in ε. Then, we have:

$$X_t = X_t^* + e_t^* = c(L)\varepsilon_t + e_t^*, \tag{a.5}$$

where the process (e_t^*) is uncorrelated with any nonlinear transformations of (ε_t). We get a weak linear two-sided moving average representation of the process in (ε, e^*), where the ε_t variables are i.i.d., but the e_t^* variables are only uncorrelated. Equivalently, the process (X_t) is such that:

$$(1-\alpha L)(1-\beta L^{-1})X_t = \varepsilon_t + (1-\alpha L)(1-\beta L^{-1})e_t^* \equiv e_t,$$

where the aggregate shock e_t depends on ε_t, e_t^* and is not a strong white noise, due to the properties of $(\varepsilon_t), (e_t^*)$. Since

$$e_t = (1+\alpha\beta)X_t - \beta X_{t+1} - \alpha X_{t-1},$$

we have by (a.2):

$$\begin{aligned} e_t = \quad & (1+\alpha\beta)[\varepsilon_t + \sum_k \varepsilon_{t-k}(t) + \sum_k \varepsilon_{t+k}(t)] \\ & -\beta[\varepsilon_{t+1} + \sum_k \varepsilon_{t+1-k}(t+1) + \sum_k \varepsilon_{t+1+k}(t+1)] \\ & -\alpha[\varepsilon_{t-1} + \sum_k \varepsilon_{t-1-k}(t-1) + \sum_k \varepsilon_{t-1+k}(t-1)] \end{aligned}$$

where $\varepsilon_{t-k}(t)$ [resp. $\varepsilon_{t+k}(t)$] depends on ε_t and on Z. In particular,it depends on α [resp. β].

In fact, e_t is a nonlinear function of (ε, Z) that we will now show explicitly. By definition, we have:

$$\begin{aligned} e_t = \quad & (1+\alpha\beta)\varepsilon_t - \beta\varepsilon_t(t+1) - \alpha\varepsilon_t(t-1) \\ & +(1+\alpha\beta)\sum_k \varepsilon_{t-k}(t) - \beta\sum_k \varepsilon_{t-k}(t+1) - \alpha\sum_k \varepsilon_{t-k}(t-1) \\ & +(1+\alpha\beta)\sum_k \varepsilon_{t+k}(t) - \beta\sum_k \varepsilon_{t+k}(t+1) - \alpha\sum_k \varepsilon_{t+k}(t-1), \end{aligned}$$

because the terms $-\beta\varepsilon_{t+1} - \alpha\varepsilon_{t-1}$ are already included in the sums of lines 2 and 3, and the terms $-\beta\varepsilon_t(t+1) - \alpha\varepsilon_t(t-1)$ are not accounted for in those sums and have to be added.

Based on the MA(∞) representation (a.1), we have:

$$\begin{aligned} E_\theta(e_t|\varepsilon) = \quad & (1+\alpha\beta)\varepsilon_t - \beta\varepsilon_t(t+1) - \alpha\varepsilon_t(t-1) \\ & +(1+\alpha\beta)[\varepsilon_{t-1}(t) + \varepsilon_{t-2}(t) + \varepsilon_{t-3}(t) + \cdots] \\ & -\beta[\varepsilon_{t-1}(t+1) + \varepsilon_{t-2}(t+1) + \varepsilon_{t-3}(t+1) + \cdots] \\ & -\alpha[\varepsilon_{t-1}(t-1) + \varepsilon_{t-2}(t-1) + \varepsilon_{t-3}(t-1) + \cdots] \\ & +(1+\alpha\beta)[\varepsilon_{t+1}(t) + \varepsilon_{t+2}(t) + \varepsilon_{t+3}(t) + \cdots] \\ & -\beta[\varepsilon_{t+1}(t+1) + \varepsilon_{t+2}(t+1) + \varepsilon_{t+3}(t+1) + \cdots] \\ & -\alpha[\varepsilon_{t+1}(t-1) + \varepsilon_{t+2}(t-1) + \varepsilon_{t+3}(t-1) + \cdots] \end{aligned}$$

Then, under the expectation conditional on ε, we have:

$$\begin{aligned} E_\theta(e_t|\varepsilon) = \quad & (1+\alpha\beta)\varepsilon_t - \beta\alpha\varepsilon_t - \alpha\beta\varepsilon_t \\ & +(1+\alpha\beta)[\alpha\varepsilon_{t-1} + \alpha^2\varepsilon_{t-2} + \alpha^3\varepsilon_{t-3} + \cdots] \\ & -\beta[\alpha^2\varepsilon_{t-1} + \alpha^3\varepsilon_{t-2} + \alpha^4\varepsilon_{t-3} + \cdots] \\ & -\alpha[\varepsilon_{t-1} + \alpha\varepsilon_{t-2} + \alpha^2\varepsilon_{t-3} + \cdots] \\ & +(1+\alpha\beta)[\beta\varepsilon_{t+1} + \beta^2\varepsilon_{t+2} + \beta^3\varepsilon_{t+3} + \cdots] \\ & -\beta[\varepsilon_{t+1} + \beta\varepsilon_{t+2} + \beta^2\varepsilon_{t+3} + \cdots] \\ & -\alpha[\beta^2\varepsilon_{t+1} + \beta^3\varepsilon_{t+2} + \beta^4\varepsilon_{t+3} + \cdots] \end{aligned}$$

We write it as:

$$\begin{aligned} E_\theta(e_t|\varepsilon) = \quad & (1+\alpha\beta)\frac{\alpha L}{1-\alpha L}\varepsilon_t - \beta\frac{\alpha^2 L}{1-\alpha L}\varepsilon_t - \alpha\frac{L}{1-\alpha L}\varepsilon_t \\ & +(1+\alpha\beta)\frac{\beta L^{-1}}{1-\beta L^{-1}}\varepsilon_t - \psi\frac{L^{-1}}{1-\beta L^{-1}}\varepsilon_t - \phi\frac{\beta^2 L^{-1}}{1-\beta L^{-1}}\varepsilon_t + (1+\alpha\beta)\varepsilon_t - \beta\alpha\varepsilon_t - \alpha\beta\varepsilon_t \end{aligned}$$

which yields

$$E_\theta(e_t|\varepsilon) = [\frac{(1+\alpha\beta)\alpha - \beta\alpha^2 - \alpha}{1-\alpha L}L + \frac{(1+\alpha\beta)\beta - \alpha\beta^2 - \beta}{1-\beta L^{-1}}L^{-1} + (1+\alpha\beta) - \beta\alpha - \alpha\beta]\varepsilon_t$$

The first two terms in the brackets simplify. Then $E_\theta(e_t|\varepsilon) = [1-\alpha\beta]\varepsilon_t$

A.2 Identification of the dynamic parameters α, β

From Proposition 5 in Pei et al. (2025) it follows that:

$$E(u^{X_t} v^{X_{t+1}}) = G_1(u(\alpha v + (1-\alpha))G_2(v(\beta u + (1-\beta)) \tag{a.6}$$

We observe that depending on functions G_1 and G_2 this function can be symmetric in the two arguments u and v, i.e., $E(u^{X_t} v^{X_{t+1}}) = E(u^{X_{t+1}} v^{X_t})$. Then, (X_t, X_{t+1}) has the same distribution as (X_{t+1}, X_t), and process (X_t) is time reversible. In such a case the dynamic parameters α and β cannot be distinguished from one another from the cross-moments, such as:

$$\begin{aligned} E(X_t X_{t+1}) &= E\exp(uX_t + vX_{t+1}) = E[(\exp u)^{X_t}(\exp v)^{X_{t+1}}] \\ &= G_1[\exp u(\alpha \exp v + 1 - \alpha)]G_2[\exp v(\beta\exp u + 1 - \beta)] \\ E\exp(uX_t + vX_{t+1}) &= 1 + uE(X_t) + vE(X_{t+1}) + \frac{1}{2}(u,v)\begin{pmatrix} EX_t^2 & EX_tX_{t+1} \\ EX_tX_{t-1} & EX_{t+1}^2 \end{pmatrix}\begin{pmatrix} u \\ v \end{pmatrix} \\ &\approx G_1[(1+u+\frac{u^2}{2})(\alpha(1+v+\frac{v^2}{2}) + (1-\alpha)]G_2[(1+v+\frac{v^2}{2})(\beta(1+u+\frac{u^2}{2}) + (1-\beta)] \end{aligned}$$

where the functions G_1, G_2 are given in Pei et al. (2025).

In Example 1, Section 3.1 Pei et al. (2025) consider G_1, G_2 for the MIAR with Poisson distributed errors with parameter λ. We get:

$$\begin{aligned} & \exp[\lambda(\frac{\alpha}{1-\alpha} + \frac{\beta}{1-\beta})\exp(u+v) + \lambda(\exp u + \exp v - \frac{\alpha}{1-\alpha} - \frac{\beta}{1-\beta}] \\ \approx \quad & \exp\left\{\lambda[(\frac{\alpha}{1-\alpha} + \frac{\beta}{1-\beta})(1+u+v+\frac{u^2}{2}+\frac{v^2}{2}+uv)] + \lambda[(1+u+\frac{u^2}{2}+1+v+\frac{v^2}{2}) - \frac{1}{1-\alpha} - \frac{1}{1-\beta}]\right\} \end{aligned}$$

using $\exp(uX) = 1 + uX + \frac{u^2}{2}X^2 + ...$ We observe that it can be approximated as:

$$\begin{aligned} & 1 + \lambda(\frac{\alpha}{1-\alpha} + \frac{\beta}{1-\beta})(1+u+v+\frac{u^2}{2}+\frac{v^2}{2}+uv) \\ + \quad & \lambda[(1+u+\frac{u^2}{2}+1+v+\frac{v^2}{2}) - \frac{\alpha}{1-\alpha} - \frac{\beta}{1-\beta}] \\ + \quad & \frac{1}{2}[\lambda(\frac{\alpha}{1-\alpha} + \frac{\beta}{1-\beta})(1+u+v+\frac{u^2}{2}+\frac{v^2}{2}+uv) + \lambda[(1+u+\frac{u^2}{2}+1+v+\frac{v^2}{2}) - \frac{\alpha}{1-\alpha} - \frac{\beta}{1-\beta}]]^2 \\ \approx \quad & uv\lambda(\frac{\alpha}{1-\alpha} + \frac{\beta}{1-\beta}) + \frac{1}{2}4\lambda^2(\frac{\alpha}{1-\alpha} + \frac{\beta}{1-\beta})^2 uv + 2\lambda^2(uv) + 2\lambda^2(\frac{\alpha}{1-\alpha} + \frac{\beta}{1-\beta})3uv \end{aligned}$$

We conclude that:

$$E(X_t X_{t+1}) = 2\lambda(\frac{\alpha}{1-\alpha} + \frac{\beta}{1-\beta}) + 4\lambda^2(\frac{\alpha}{1-\alpha} + \frac{\beta}{1-\beta})^2 + 4\lambda^2 + 12\lambda^2((\frac{\alpha}{1-\alpha} + \frac{\beta}{1-\beta})$$

and observe that the cross-moment is symmetric in α and β, which is consistent with the conclusion of Pei et al. (2025) that the MIAR with Poisson distributed errors is time reversible. Therefore, the forward and backward dynamics cannot be distinguished in this process.

In contrast, the MIAR with $\mathcal{NB}(n, p)$ distributed errors and with discrete stable errors, given in Examples 2 and 3 of Pei et al. (2025) are time irreversible. For these processes, function (a.1) is asymmetric in u and v when $\alpha \neq \beta$. We have the cross-moment:

$$\begin{aligned} E(X_t X_{t+1}) = & \left\{ \prod_{k=0}^{\infty} \frac{p_n}{[1-(1-p)(1-\alpha^k) - \alpha^k(1-p)A]^n} \right\} \\ & \times \left\{ \prod_{k=0}^{\infty} \frac{p_n}{[1-(1-p)(1-\beta^k) - \beta^k(1-p)B]^n} \right\} \end{aligned}$$

where $A = \exp u(\alpha \exp v + 1 - \alpha)]$ and $B = \exp v(\beta \exp u + 1 - \beta)]$. This cross-product is asymmetric in u, v for $\alpha \neq \beta$. It is also asymmetric in α, β when $u \neq v$. This allows for identifying the dynamics by considering $E(X_t X_{t+1})$ and $E(X_t X_{t+1})$.

A.3 Autocovariance at lag 1 of MIAR for Poisson(λ) distributed errors

$$\begin{aligned} E(u^{X_t} v^{X_{t+1}}) &= G_1(u(\alpha v + (1-\alpha))G_2(v(\beta u + (1-\beta)) \\ E(X_t X_{t+1}) &= E \exp(u X_t + v X_{t+1}) = E[(\exp u)^{X_t} (\exp v)^{X_{t+1}}] \\ &= G_1[\exp u(\alpha \exp v + 1 - \alpha)] G_2[\exp v(\beta \exp u + 1 - \beta)] \\ E \exp(u X_t + v X_{t+1}) &= 1 + u E(X_t) + v E(X_{t+1}) + \frac{1}{2}(u, v) \begin{pmatrix} E X_t^2 & E X_t X_{t+1} \\ E X_t X_{t-1} & E X_{t+1}^2 \end{pmatrix} \begin{pmatrix} u \\ v \end{pmatrix} \\ & \approx G_1[(1 + u + \frac{u^2}{2})(\alpha(1 + v + \frac{v^2}{2}) + (1-\alpha)] G_2[(1 + v + \frac{v^2}{2})(\beta(1 + u + \frac{u^2}{2}) + (1-\beta)] \end{aligned}$$

where the functions G_1, G_2 are given in Pei et al. (2025) in Example 1, Section 3.1. We get:

$$\begin{aligned} & \exp[\lambda(\frac{\alpha}{1-\alpha} + \frac{\beta}{1-\beta}) \exp(u+v) + \lambda(\exp u + \exp v - \frac{\alpha}{1-\alpha} - \frac{\beta}{1-\beta}] \\ \approx \quad & \exp \left\{ \lambda[(\frac{\alpha}{1-\alpha} + \frac{\beta}{1-\beta})(1 + u + v + \frac{u^2}{2} + \frac{v^2}{2} + uv)] + \lambda[(1 + u + \frac{u^2}{2} + 1 + v + \frac{v^2}{2}) - \frac{1}{1-\alpha} - \frac{1}{1-\beta}] \right\} \end{aligned}$$

using $\exp(uX) = 1 + uX + \frac{u^2}{2} X^2 + ...$ We observe that it can be approximated as:

$$
\begin{aligned}
& 1+\lambda(\frac{\alpha}{1-\alpha}+\frac{\beta}{1-\beta})(1+u+v+\frac{u^2}{2}+\frac{v^2}{2}+uv) \\
+ \quad & \lambda[(1+u+\frac{u^2}{2}+1+v+\frac{v^2}{2})-\frac{\alpha}{1-\alpha}-\frac{\beta}{1-\beta}] \\
+ \quad & \frac{1}{2}[\lambda(\frac{\alpha}{1-\alpha}+\frac{\beta}{1-\beta})(1+u+v+\frac{u^2}{2}+\frac{v^2}{2}+uv)+\lambda[(1+u+\frac{u^2}{2}+1+v+\frac{v^2}{2})-\frac{\alpha}{1-\alpha}-\frac{\beta}{1-\beta}]]^2 \\
\approx \quad & uv\lambda(\frac{\alpha}{1-\alpha}+\frac{\beta}{1-\beta})+\frac{1}{2}4\lambda^2(\frac{\alpha}{1-\alpha}+\frac{\beta}{1-\beta})^2uv+2\lambda^2(uv)+2\lambda^2(\frac{\alpha}{1-\alpha}+\frac{\beta}{1-\beta})3uv
\end{aligned}
$$

We conclude that:

$$E(X_tX_{t+1})=2\lambda(\frac{\alpha}{1-\alpha}+\frac{\beta}{1-\beta})+4\lambda^2(\frac{\alpha}{1-\alpha}+\frac{\beta}{1-\beta})^2+4\lambda^2+12\lambda^2((\frac{\alpha}{1-\alpha}+\frac{\beta}{1-\beta})$$

is symmetric with respect to α and β.

B.1 Distribution of Data

1) The numbers of negative tweets of apple Inc. stock

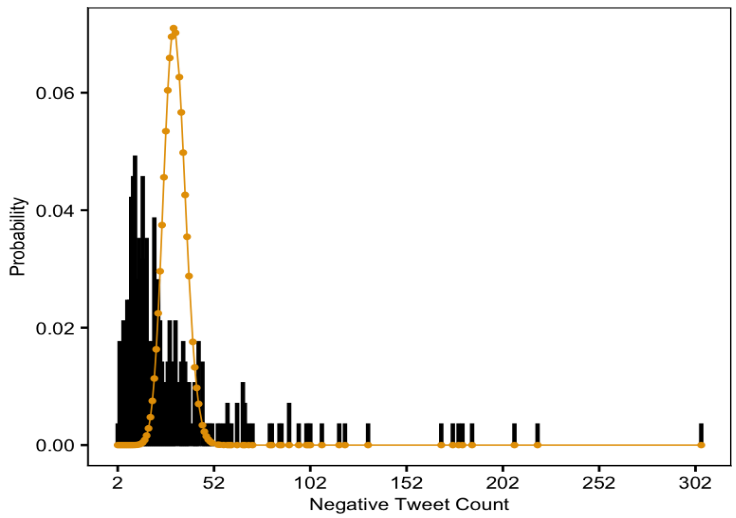

Figure 6: Distribution of AAPL negative tweets dataset(black bars), Poisson distribution(orange line)

2) The numbers of negative tweets of GameStop stock

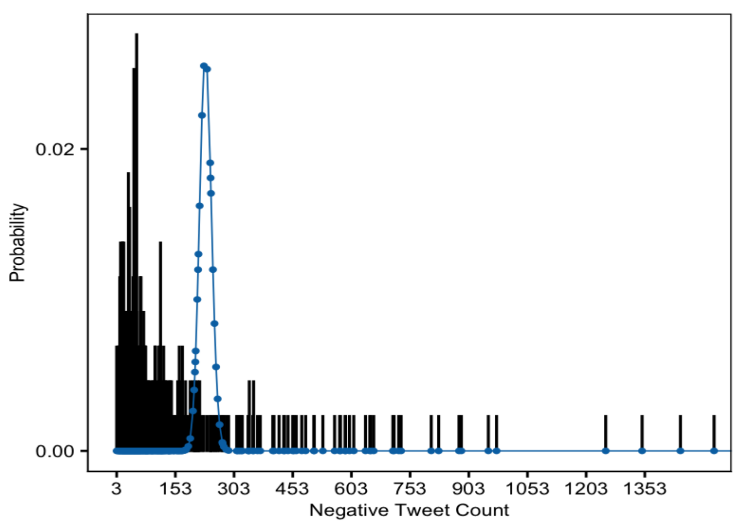

Figure 7: Distribution of GME negative tweets dataset(black bars), Poisson distribution(blue line)

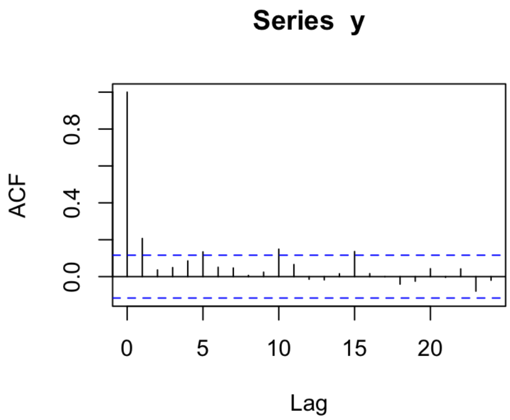

(a) ACF the negative tweets of AAPLE

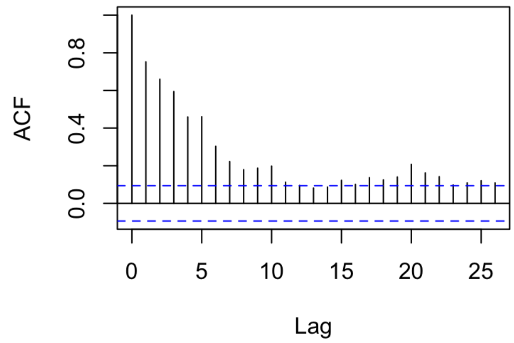

(b) ACF the negative tweets of GME

Figure 8: ACF plots of Raw data

B.2 Additional Empirical Results

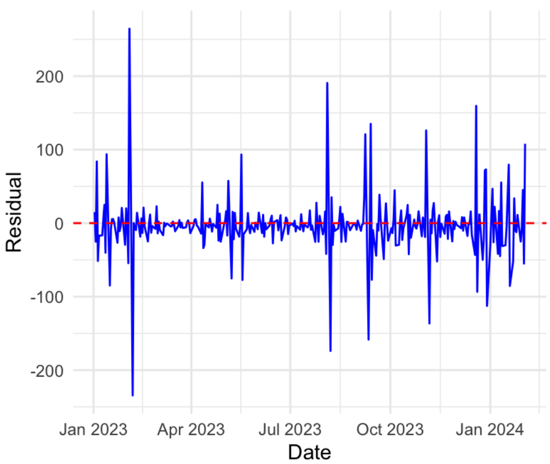

(a) Residuals over time

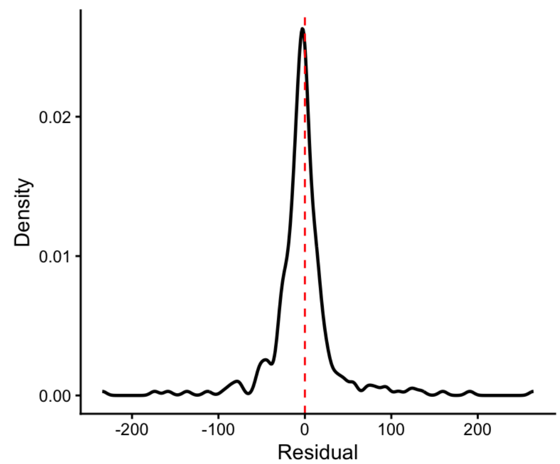

(b) Density of residuals

Figure 9: Residual diagnostics for the MIAR(1,1) model- AAPL dataset